SLL
P
IL

SLL 82-266/P

Breakdown At High Overvoltages

E. E. Kunhardt

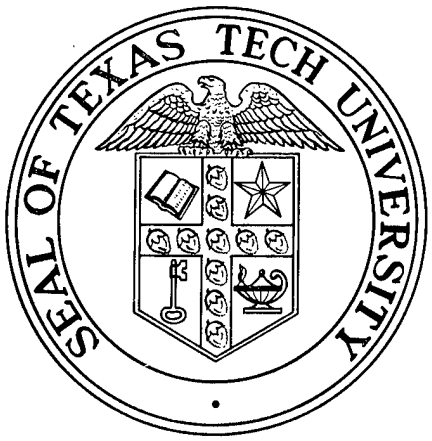

November 15, 1980

IONIZED GAS LABORATORY

DEPARTMENT OF ELECTRICAL ENGINEERING

TEXAS TECH UNIVERSITY

Lubbock, Texas 79409

U3811

Accession Number: 3811

Publication Date: Oct 28, 1980

Title: Breakdown at High Overvoltages

Personal Author: Kunhardt, E.E.

Corporate Author Or Publisher: Ionized Gas Laboratory, Box 4439, Texas Tech University, Lubbock, TX 7

Report Prepared for: Naval Surface Weapons Center - Code F12, Dahlgren, VA 22448 Report Number Assigned by Contract Monitor: SLL 82 266

Comments on Document: Archive, RRI, DEW.

Descriptors, Keywords: Directed Energy Weapon DEW Breakdown High Overvoltage Electron Kinetics Inhomogeneous Electric Field Time Lag Measurement Theory Experiment Model Townsend Avalnche Mechanism Power Laser Low Inductanc

Pages: 61

Cataloged Date: Oct 19, 1992

Contract Number: N60921-79-C-A187

Document Type: HC

Number of Copies In Library: 000001

Record ID: 24997

Source of Document: DEW

Research and Development Final Report

on

Breakdown at High Overvoltages

E. E. Kunhardt
Electrical Engineering Department
Texas Tech University
Lubbock, Texas 79409

Sponsored by

Defense Advanced Research Projects Agency (DOD)
ARPA Order No. 3763
Monitored by Naval Air Systems Command
(Dr. Richard J. Wasneski, AIR 350F)

and

Naval Surface Weapons Center (Code F12)
Under Contract #N60921-79-C-A187

SECURITY CLASSIFICATION OF THIS PAGE *(When Data Entered)*

REPORT DOCUMENTATION PAGE		READ INSTRUCTIONS BEFORE COMPLETING FORM
1. REPORT NUMBER Final Report	2. GOVT ACCESSION NO.	3. RECIPIENT'S CATALOG NUMBER
4. TITLE *(and Subtitle)* Breakdown at High Overvoltages		5. TYPE OF REPORT & PERIOD COVERED Final Report May 1,1979-Sept.30, 1980
		6. PERFORMING ORG. REPORT NUMBER
7. AUTHOR(s) E. E. Kunhardt		8. CONTRACT OR GRANT NUMBER(s) N60921-79C-A187
9. PERFORMING ORGANIZATION NAME AND ADDRESS Ionized Gas Laboratory Box 4439 Texas Tech University, Lubbock, TX 79409		10. PROGRAM ELEMENT, PROJECT, TASK AREA & WORK UNIT NUMBERS
11. CONTROLLING OFFICE NAME AND ADDRESS Naval Surface Weapons Center - Code F12 Dahlgren, VA 22448		12. REPORT DATE October 28, 1980 13. NUMBER OF PAGES 61
14. MONITORING AGENCY NAME & ADDRESS*(if different from Controlling Office)*		15. SECURITY CLASS. *(of this report)* Unclassified 15a. DECLASSIFICATION/DOWNGRADING SCHEDULE

16. DISTRIBUTION STATEMENT *(of this Report)*
Distribution Unlimited

17. DISTRIBUTION STATEMENT *(of the abstract entered in Block 20, if different from Report)*

18. SUPPLEMENTARY NOTES

19. KEY WORDS *(Continue on reverse side if necessary and identify by block number)*
Breakdown at High overvoltage
Electron Kinetics in inhomogeneous Electric Fields
Time lag measurements

20. ABSTRACT *(Continue on reverse side if necessary and identify by block number)*
A theoretical and experimental investigation of the mechanisms via which a gas, at high pressures, undergoes electrical breakdown has been carried out.

Theoretically, a model has been developed to describe the initial phases of breakdown in the regime where the Townsend avalanche mechanism does not apply. The model is based on electron Kinetics in regions of highly inhomogeneous electric fields.

DD FORM 1 JAN 73 1473 EDITION OF 1 NOV 65 IS OBSOLETE

SECURITY CLASSIFICATION OF THIS PAGE *(When Data Entered)*

I. Introduction

One of the principal prerequisites in the development of high current, charged particle accelerators and high power lasers is the development of a high voltage, low inductance nanosecond switch. This requirement has led to the investigation of breakdown phenomena in high pressure, overvolted gaps. When a high voltage is applied to a parallel plate gap, containing a gas or mixture of gases, the ionization processes resulting from the creation of some initial electrons in the gap space, and the subsequent motion of the charge carriers, can cause the collapse of the voltage across the gap. Thus, the evolution of the ionization in the applied electric field, from the small number of initiatory electrons up to a final steady current, is of fundamental inportance in the development of fast, high power gas switches.

This research program is responsible for investigating, theoretically and experimentally, the gas breakdown phenomenon as a function of overvoltage (i.e. voltages above D. C. breakdown voltage) and to develop a theoretical model for the observed phenomena.

In the following sections, we discuss the findings of this study.

II. Theoretical Investigations

There is at present no agreement among researchers as to what processes are important in the breakdown phenomenon as the applied voltage is increased above selfbreakdown. As part of this program, a colloquium was given at the naval surface weapons Center, Dahlgren; in which the various theories of breakdown and the present status of the subject was reviewed. As a result, a review paper was published and is included in this report as Appendix I.

In our research effort, a model to describe the initial phase of breakdown in high pressure, overvolted, spark gaps was developed. The model offers the attractive feature of the unification of all the proposed breakdown phenomena; that is, it provides a continuous picture of the development of the initial phase of breakdown above the Townsend regime. A paper describing this model has been published. A copy is included as Appendix II. A conference paper was also given and a copy of the abstract is also included.

A mathematical formulation of the above model is in progress. The mathematical problem is basically that of solving the coupled Boltzmann-Poisson system of equations in a region of high electric field. This is to be done computationally. A major obstacle in the simulations is the computational time required to solve the Poisson equation in cylindrical coordinates. A fast alogarithm is required in order to be able to tract the development of the avalanche for a long period of time. As a result, we developed a fast alogarithm for solving Poisson's equation. The outline of a paper, which is in preparation, and the computer printout of the alogarithm (which is a subroutine in the main program) is included in Appendix III. An explanation of how the subroutine is used is also included.

III Experimental Investigations

A photograph of the facility built for the experimental study of gas breakdown at high overvoltages is shown in Fig. 1. A schematic layout of this facility is shown in Fig. 2. The setup consists of three main parts: (1) The pulse generator (a modified Heds pulser[1]), (2) the experimental chamber and (3) the diagnostic probes.

The Heds pulser is capable of producing trapezoidal voltage pulses in the range of 50 to 160 kV amplitude, with a 4 nsec risetime and a 50 nsec width, into a 52 ohm line.

The experimental chamber is a coaxial transmission line with 52 ohm characteristic impedance, terminated in a matched load. An interruption in the center conductor of the line is used as the spark gap.

The salient features of this facility are:

a) Well matched components to minimize reflections

b) Base chamber pressure in the 10^{-7} mmHg range to minimize unwanted impurities.

c) ability to use large electrode separation (up to 5 cm) while maintaining strong and relatively homogenous external electric fields.

d) direct access to either cathode or anode (depending on the polarity of the incident pulse, which can be reversed.

e) capacitive and B probes at various locations to measure incident, reflected and transmitted pulses.

Using the set up described above, we have carried out an investigation of the observational delay time, i.e. the time elapsed from the application of the voltage to the gap to the time of rapid current growth. We have obtained data of the behavior of this time lag as a function of percent overvoltage

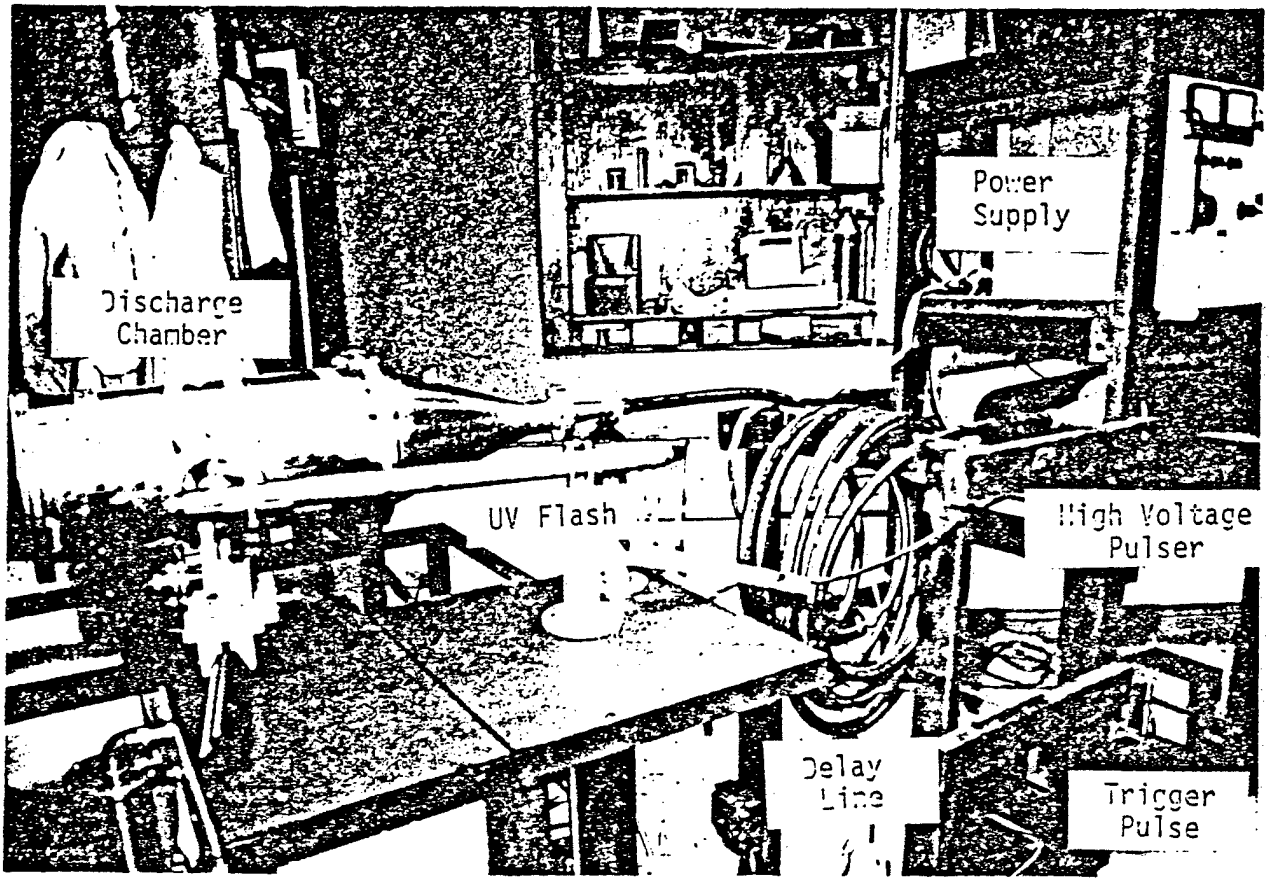

Fig. 1 View of the experimental facility

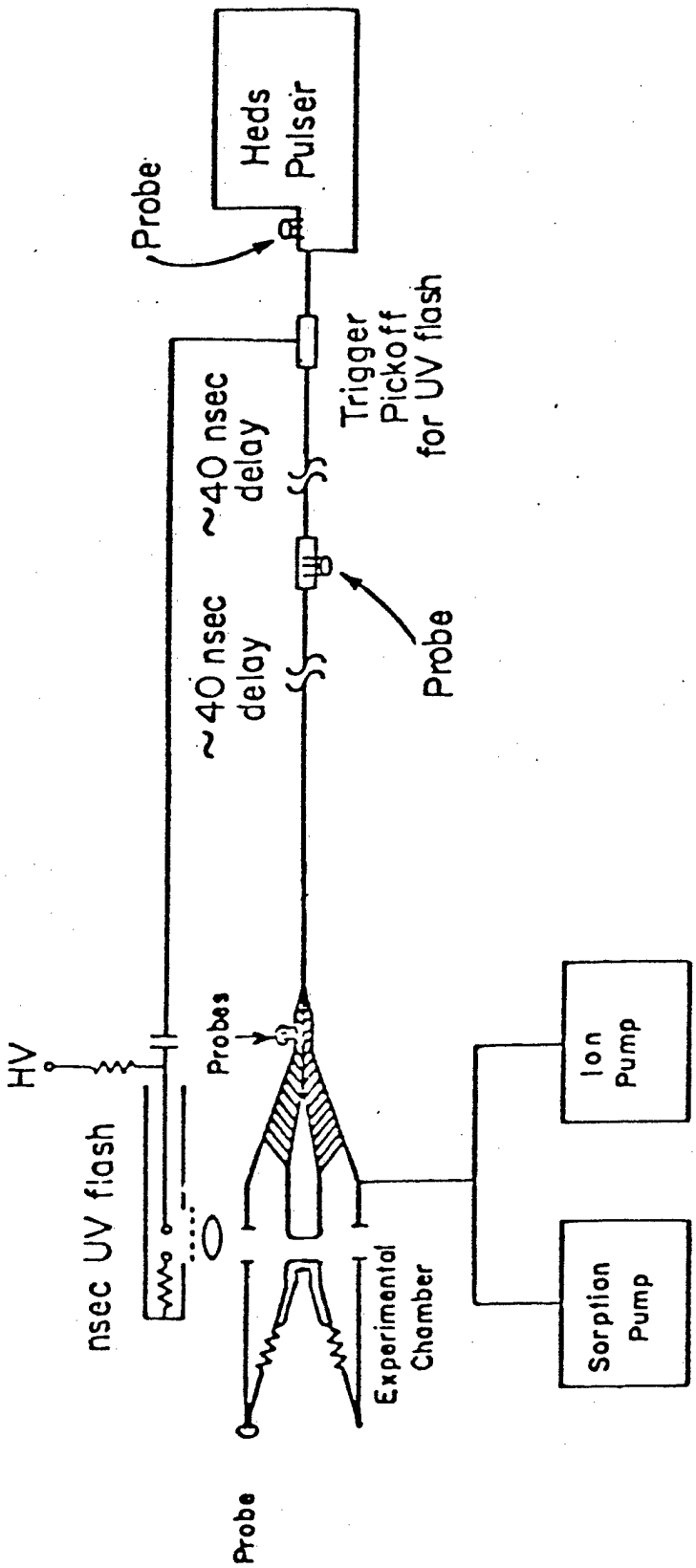

Fig. 2 Schematic of Experimental Facility.

(ranging from ∿ 10% to 1300% above D.C. breakdown), gas impurity (Technical grade nitrogen, 98% N_2, and purified nitrogen, 99.998% N_2), and pressures (ranging from 50 to 1500 torr). The experiments were carried out in a 1 cm gap, using highly polished, Rogowskii shaped, Aluminum electrodes. The observational time lag consists of the statistical time lag and the formative time lag. The role played by the statistical phenomena in these experiments is different than for small gap experiments. This is due to the fact that for our case, the inter-electrode volume (large gap separation) is large, so that there is a higher probability of having an electron present in the gap at the time the voltage is applied to the gap.

Since the percent overvoltage is a parameter of importance in our studies, a D.C. breakdown study was carried out to determine the self breakdown voltage, V_s. These experiments were done using aluminum electrodes and two types of gases: a) Technical grade Nitrogen (99.0% N_2), and b) "purified" Nitrogen (99.998% N_2). Examples of V_s vs. pd curves are shown in Fig. 3 where we also plot the results obtained by Dakin et.al.[2] D.C. Breakdown was "defined" to be the voltage at which consistent D.C. breakdown was observed. This voltage however has a very narrow distribution so that changes in the "definition" yields little difference.

In the pulse-breakdown study, for a given incident pulse, the reflected and transmitted pulses, due to the collapse of the gap, were recorded. From the transmitted pulse recordings, the observational time lag can be determined. A typical recording is shown in Fig. 4. The part of the signal indicated with an "A" is the capacitive coupled signal, and corresponds to the arrival of the incident pulse to the gap. A time later, the current rapidly increases, indicative of the complete collapse of the insulating properties of the gas. This elapsed time is the observational time lag. Since the slope of the

Fig. 3 Static Breakdown

vs

pd

EXPERIMENTAL STATIC BREAKDOWN VOLTAGES

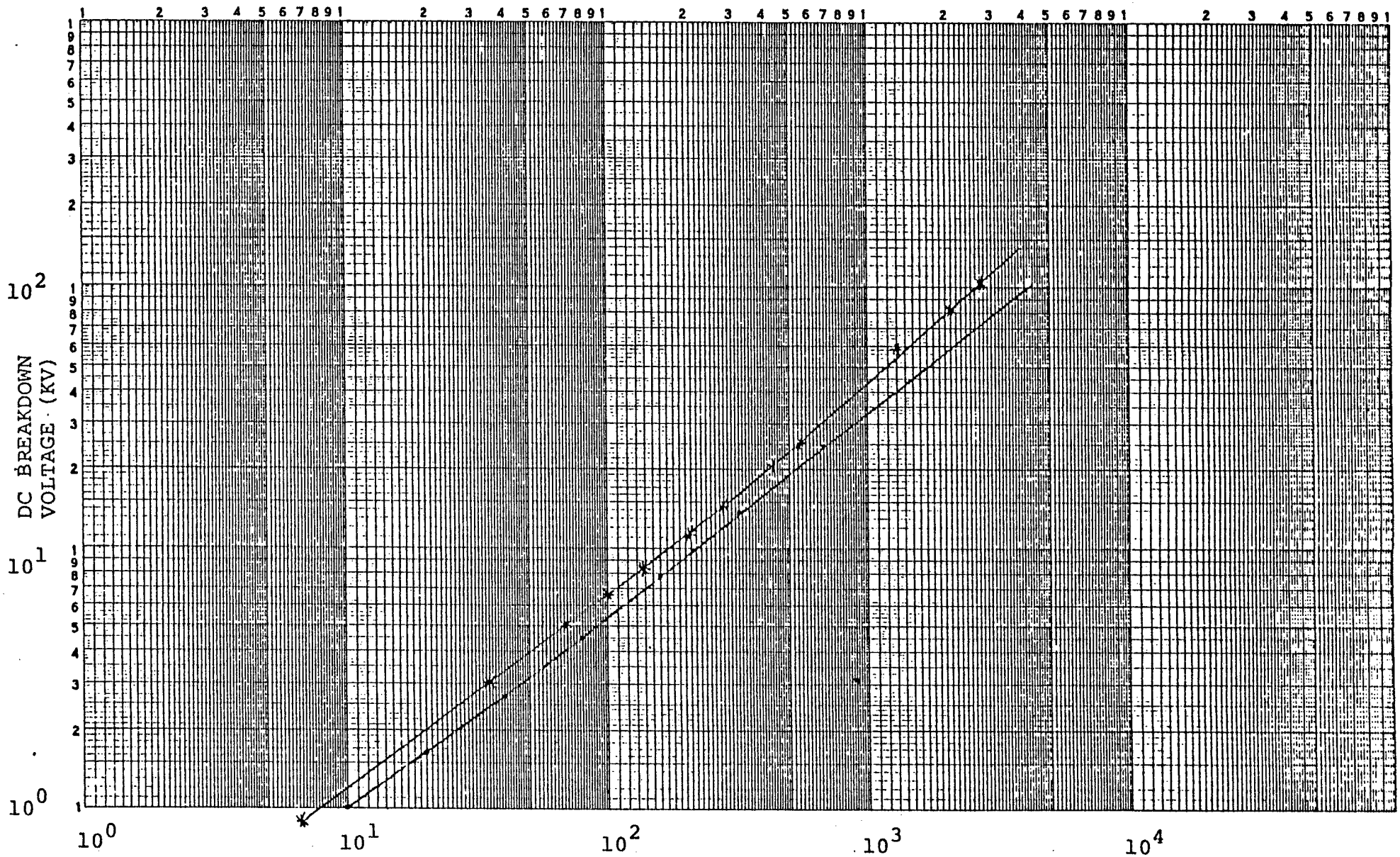

EXPERIMENTAL STATIC BREAKDOWN VOLTAGES

Impure N_2, Clean Electrodes

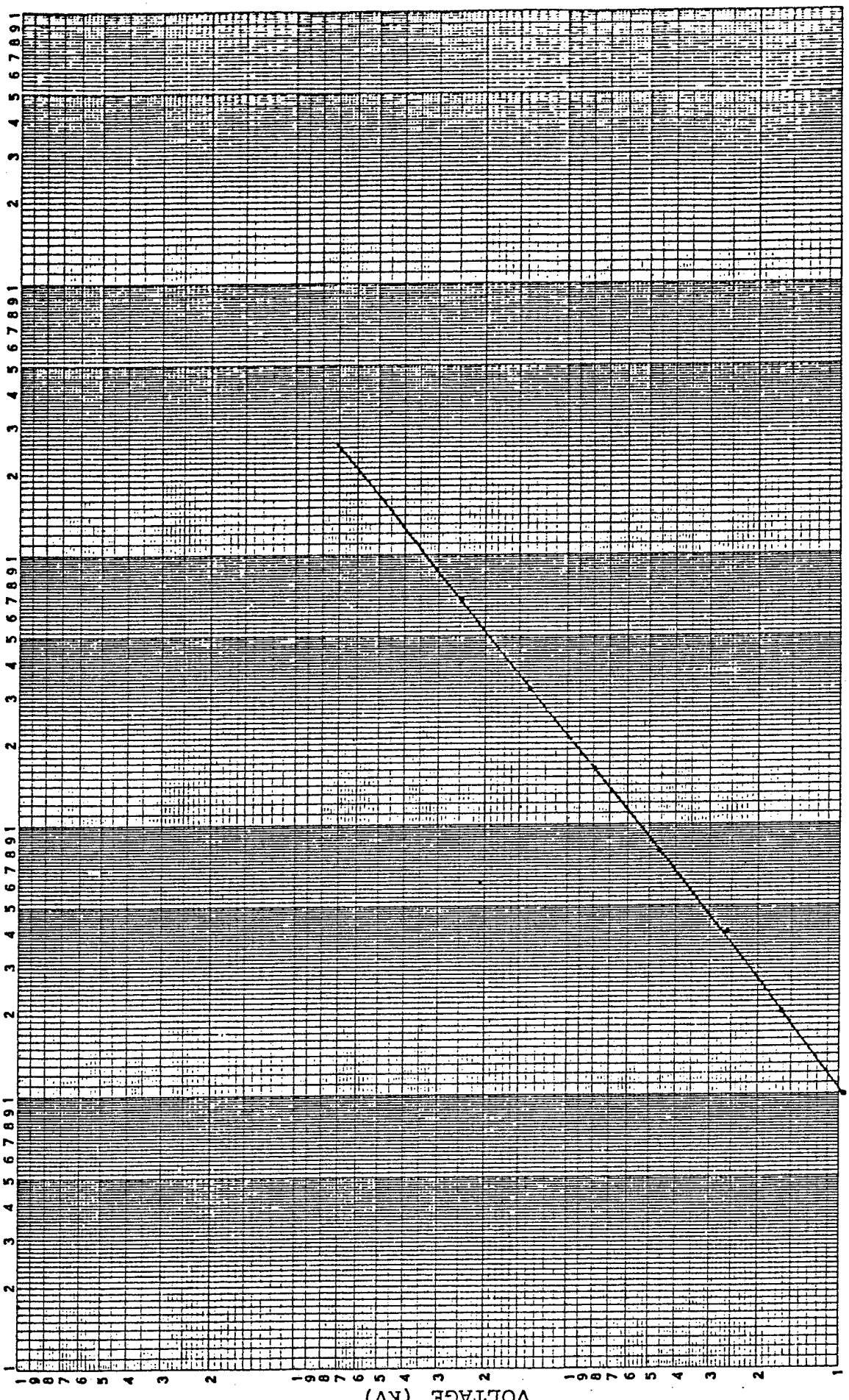

EXPERIMENTAL STATIC BREAKDOWN VOLTAGES

Pure N_2, "Dirty" Electrodes

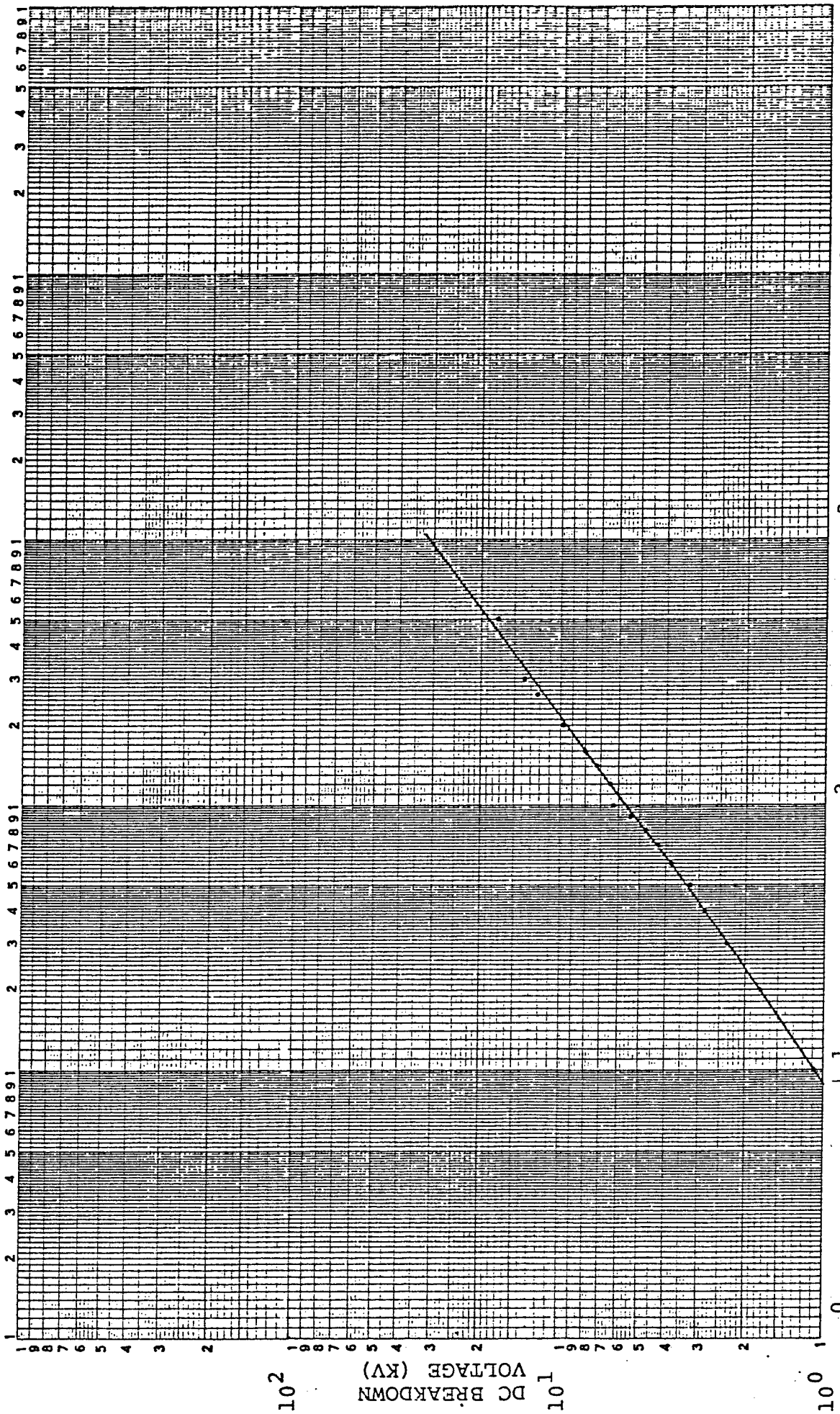

EXPERIMENTAL STATIC BREAKDOWN VOLTAGES

Impure N_2, "Dirty" Electrodes

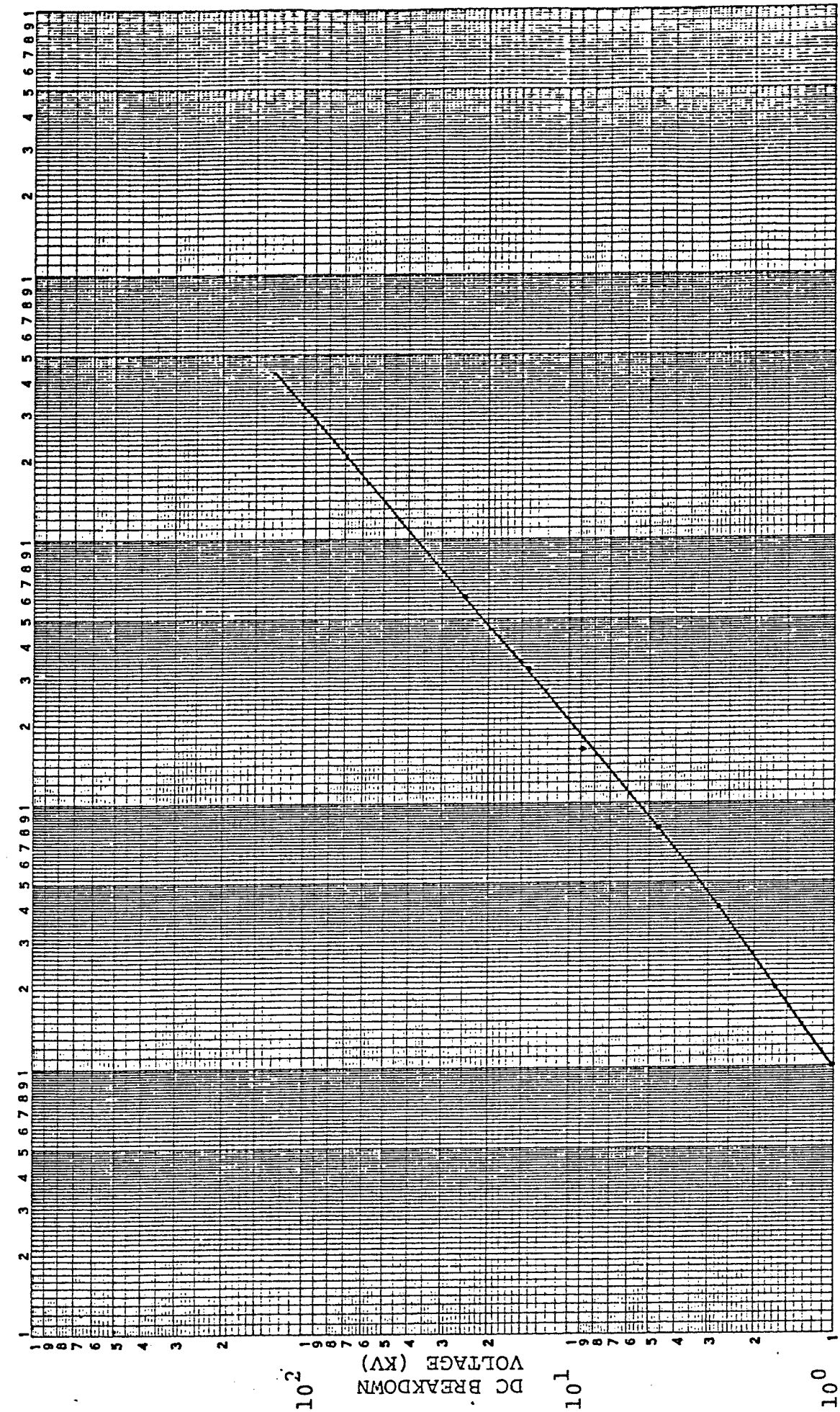

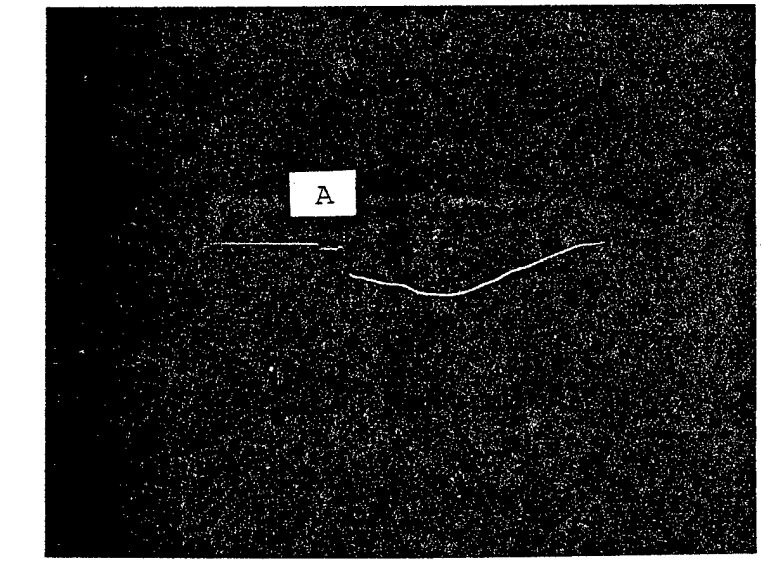

Fig. 4 Transmitted current pulse

current rise is very high, the observational time lag can be measured to within .1 nanosecond accuracy; using a Tektronix 7104 oscilloscope. An expanded display of the region "A" is shown in Fig. 5. Note that the current rise is so high that the scope cannot trace it. The tail end of the transmitted pulse can be seen on the right of the photograph.

Approximately 90 shots were taken at each operating point (i.e. for a given pressure and % overvoltage). The procedure used in gathering this data is as follows: the chamber is initially evacuated to approximately 10^{-6} Torr and then filled with N_2 to a pressure of a few Torr. At this pressure, the gap is broken down 15-20 times. The chamber is once again evacuated and back filled to the desired operating pressure. Although 15 shots might not be enough to thoroughly "clean" the electrodes, the sparks observed at the higher pressures are randomly distributed over the electrode surface indicating statistical independence. Moreover, the number of electrons emitted per second were determined to be relatively stable throughout the experiment (this point will be discussed later).

From the 90 shots taken per point, a histogram of the observational delay is compiled. A typical histogram is shown in Fig. 6. A running average delay time is also tabulated and plotted. As seen from Fig. 7, the running average delay time reaches its asymptotic value after approximately 35 shots. Obviously if the histogram is narrower, the asymptote is reached earlier.

To describe the breakdown statistics, let Idt be the probability that an electron will appear in the gap, in the time interval between t and t + dt. I is the probability per unit time that electrons are emitted from the cathode, or the emission rate (assuming all other processes that lead to electron generation are small. This point is yet to be justified in our case since we have a large interelectrode volume). Moreover, let W be the probability that

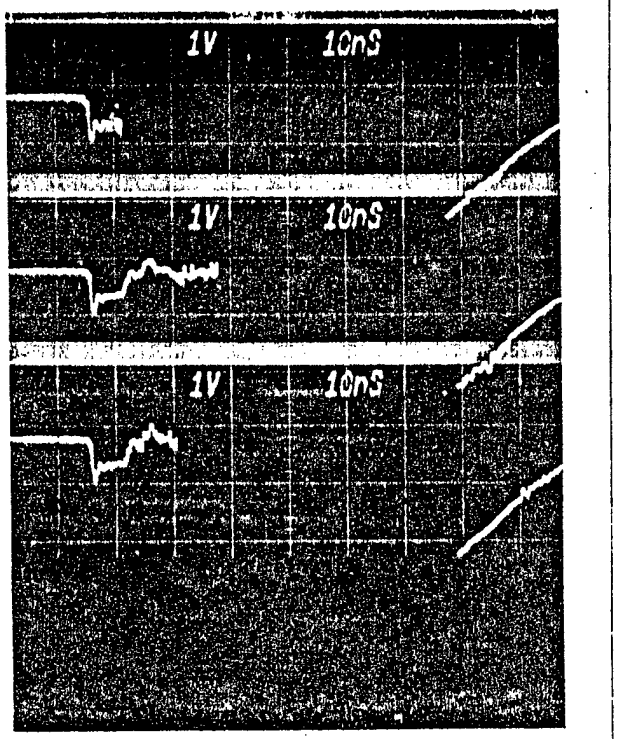

gas: Purified N_2
pressure: 100 Torr
separation: 1 cm
electrodes: Aluminum
E/N : 3724 Td

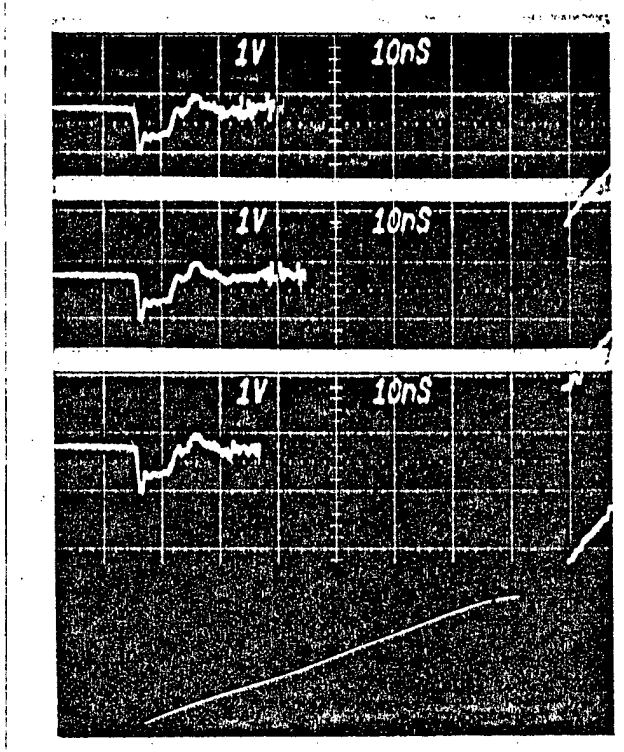

gas: Purified N_2
pressure: 150 Torr
separation: 1 cm
electrodes: Aluminum
E/N : 2482 Td

Fig. 5 Capacitive coupled signal observed prior to the colapse of the gap

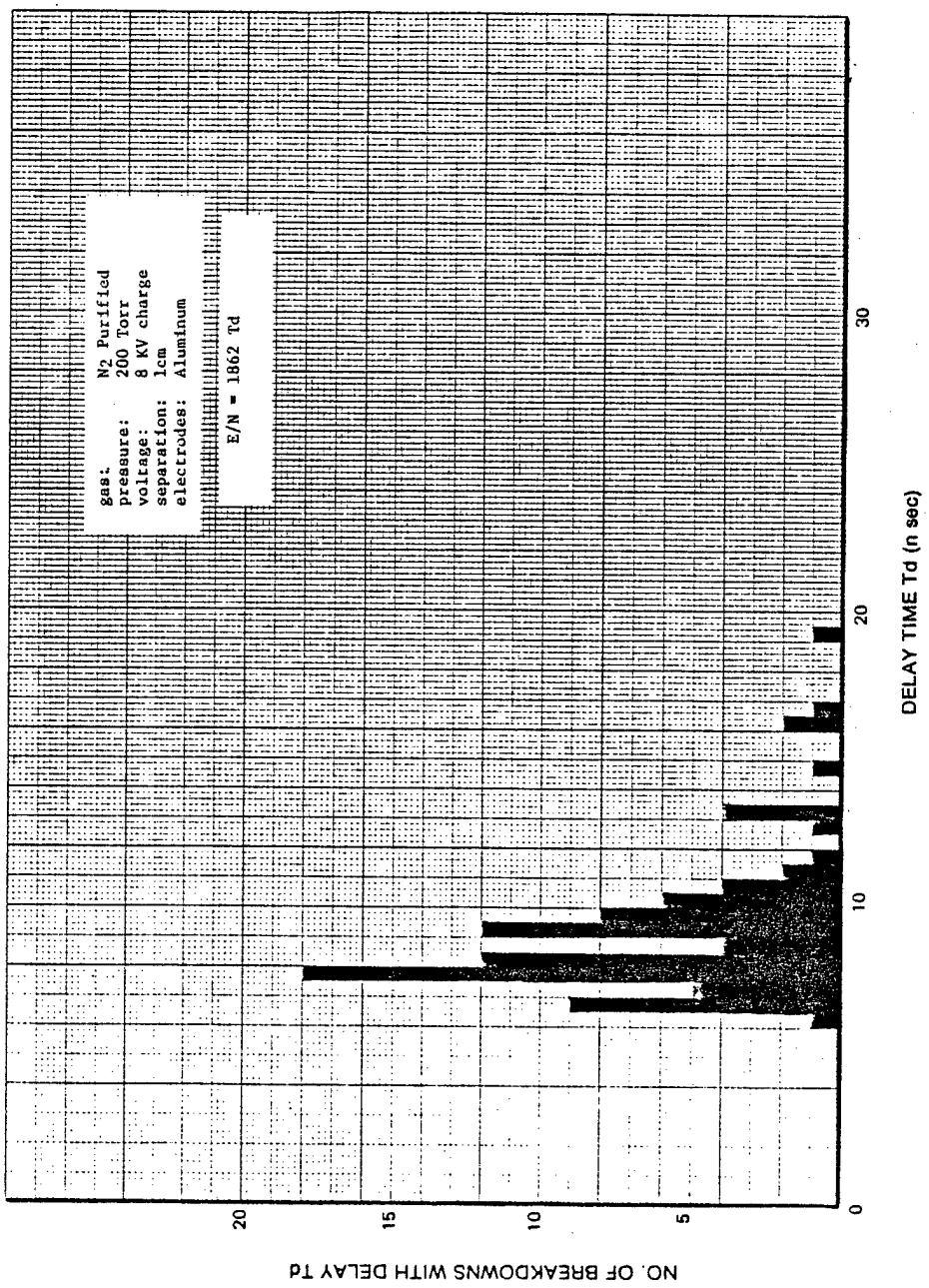

Fig. 6 Histogram of breakdown delay time

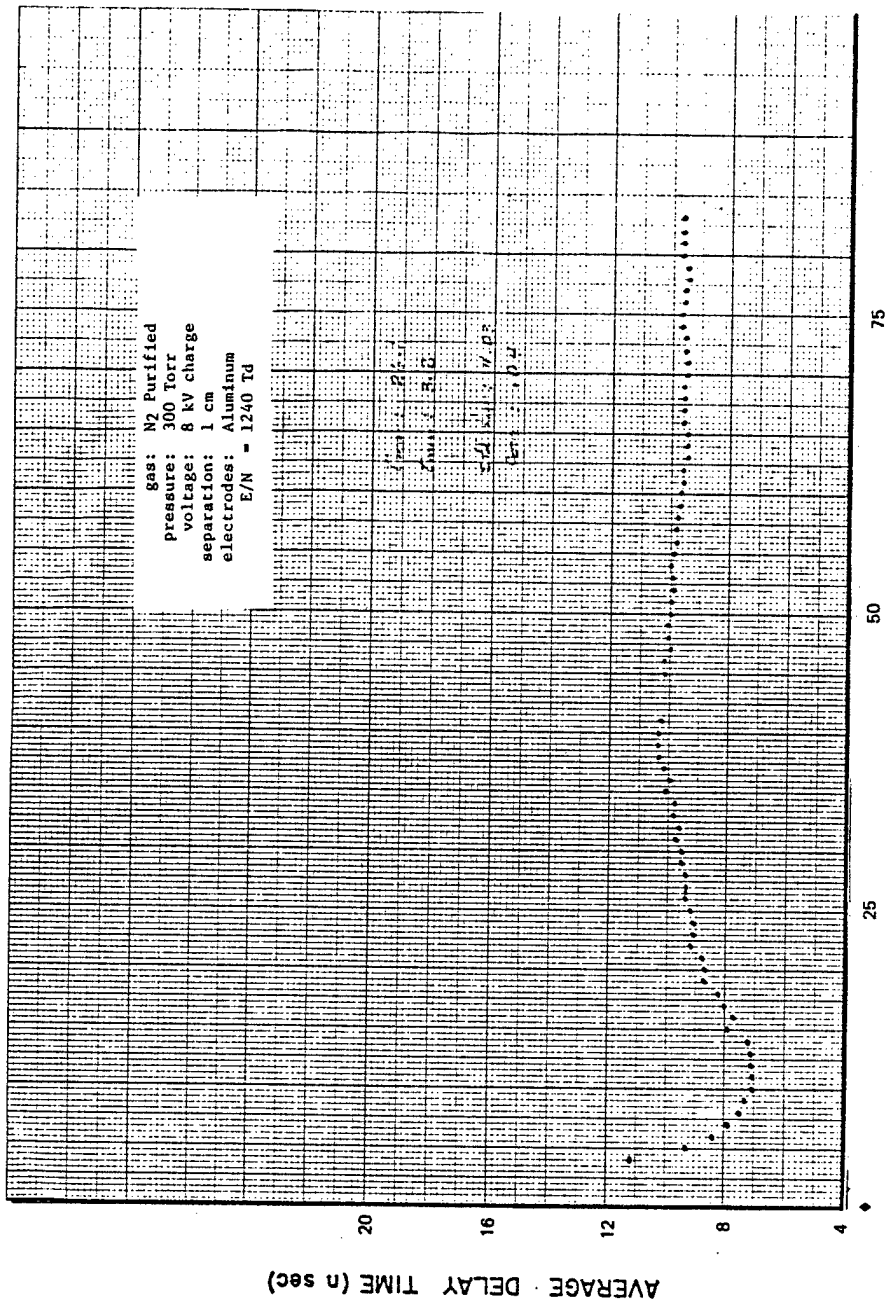

Fig. 7 Running average delay time

once an electron appears in the gap, it will lead to breakdown. These probabilities are assumed to be independent of shot number.

Knowing the above probabilities, it is then possible to calculate the probability that breakdown will occur with delay time t or greater. This can be done by noting that:

[Probability that breakdown does not occur in time t + dt] = [Probability that breakdown does not occur in time t] x [Probability it does not occur in time dt].

If P_B is this probability, then

$$P_B(t + dt) = P_B(t) [1 - WIdt]$$

expanding and integrating yields:

$$P_B(t) = e^{-WIt}$$

$P_B(t)$ can be determined experimentally as the ratio N/N_o, where N is the number of breakdowns observed to have a delay t or greater and N_o is the total number of breakdown.

Thus,

$$N/N_o = e^{-WIt}$$

or

$$|\ln (N/N_o)| = WIt$$

Therefore, a plot of the above equation will yield a straight line, whose slope is WI. Such plot is shown in Fig. 8. From this figure we determine WI to be $\simeq 5 \times 10^8$ electrons per second. If we assume that W = 1, then the cathode emission rate is 5×10^8 electrons/second.

Theoretically, the intersection of this straight line with the t axis gives the minimum delay time; i.e. the formative time lag. From Fig. 8, we note that there is a deviation of the experimental curve from a straight line. This deviation is a function of the width of the distribution. In

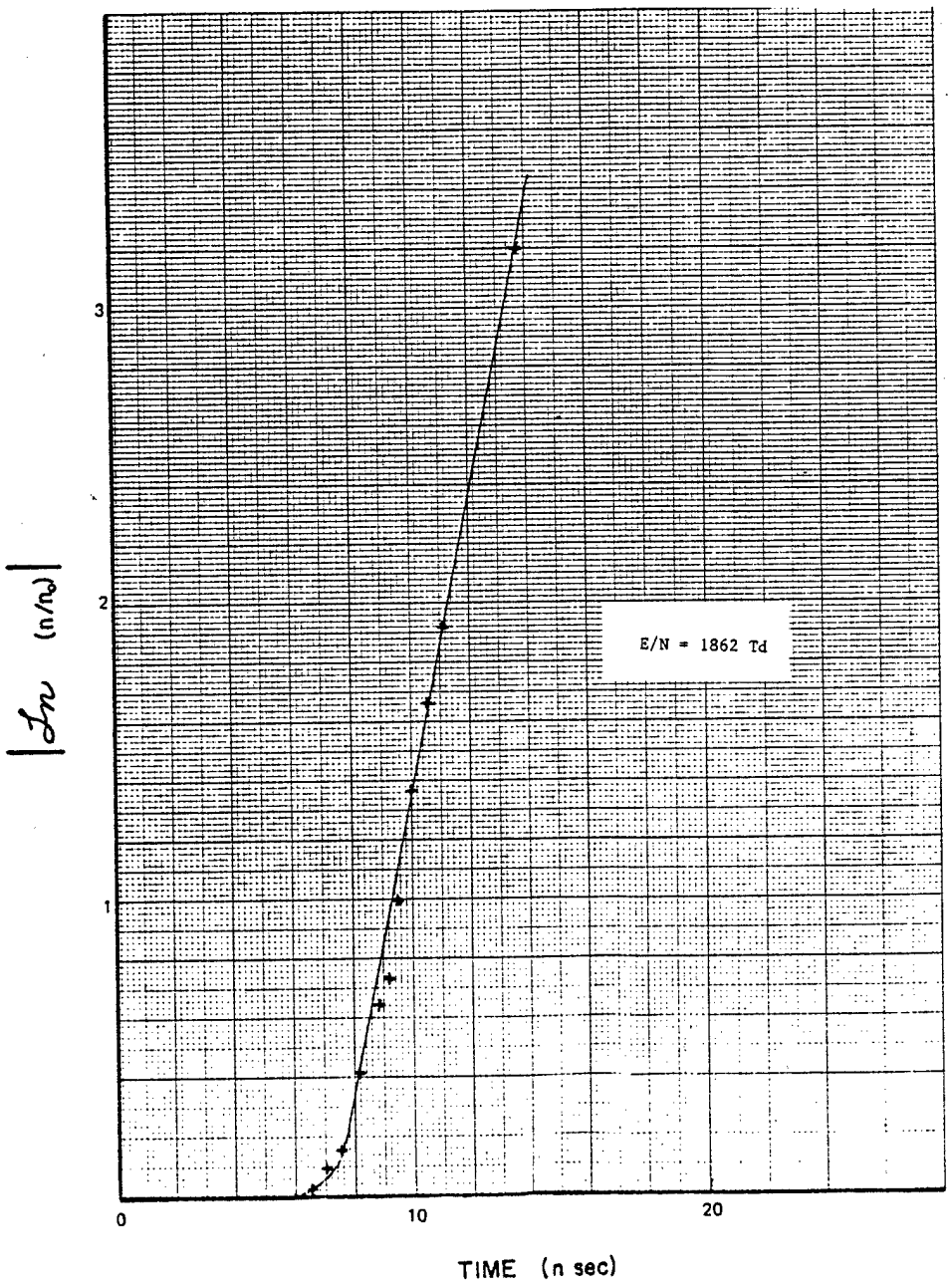

Fig. 8 Breakdown probability plot

Fig. 9, a broader distribution is shown. The corresponding Probability plot is shown in Fig. 10. Note that the deviation is greater. However, the slope of the straight section is 2.5×10^8 electrons/second which is approximately equal to that in Fig. 8. Further studies are necessary to complete the picture. Moreover, these results should be compared to small gap experiments, where I is closely associated with cathode emission, and to UV illuminated experiments where I is very large.

A plot of the average delay time as a function of percent overvoltage is shown in Fig. 11. The minimum observational time lag seems to also follow the same shape. However, further investigations are necessary to confirm this behavior.

The fact that the average delay time has a minimum as a function of percent overvoltage was rather puzzling at first. However, it can be qualitatively understood from our model. We can show that there is an optimum value of percent overvoltage for which space charge distortion of the field in the gap is maximum thus allowing for the production of "runaway" (from the avalanche head) electrons which we have postulated to be the fundamental mechanism for avalanche propagation. A quantitative analysis needs to be carried out; however, further data is necessary (i.e. UV illumination and small gap results to get a better understanding of I and W).

These results were presented at the 33rd Gaseous Electronics Conference. The abstract of the paper is included in Appendix IV.

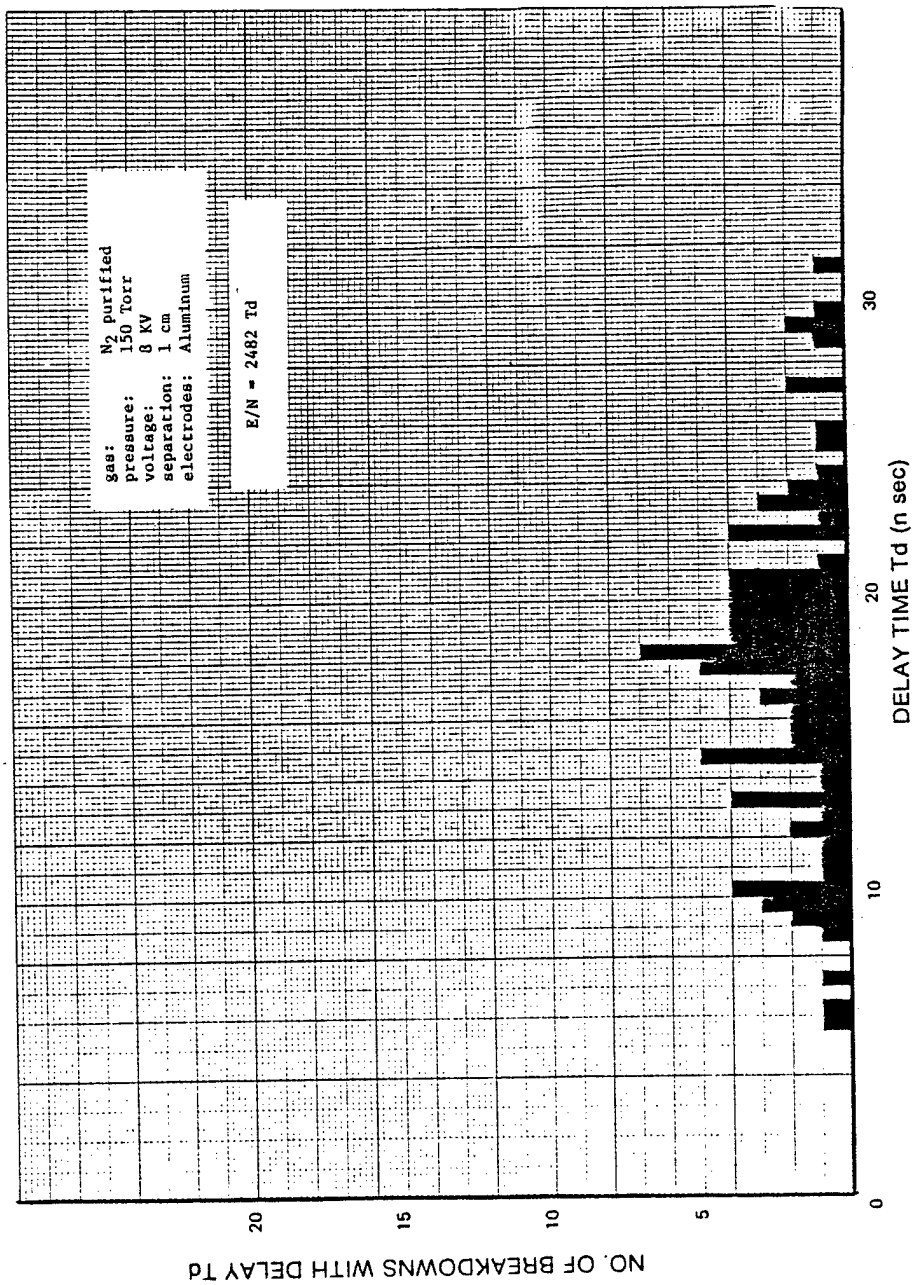

Fig. 9 Histogram of breakdown delay time

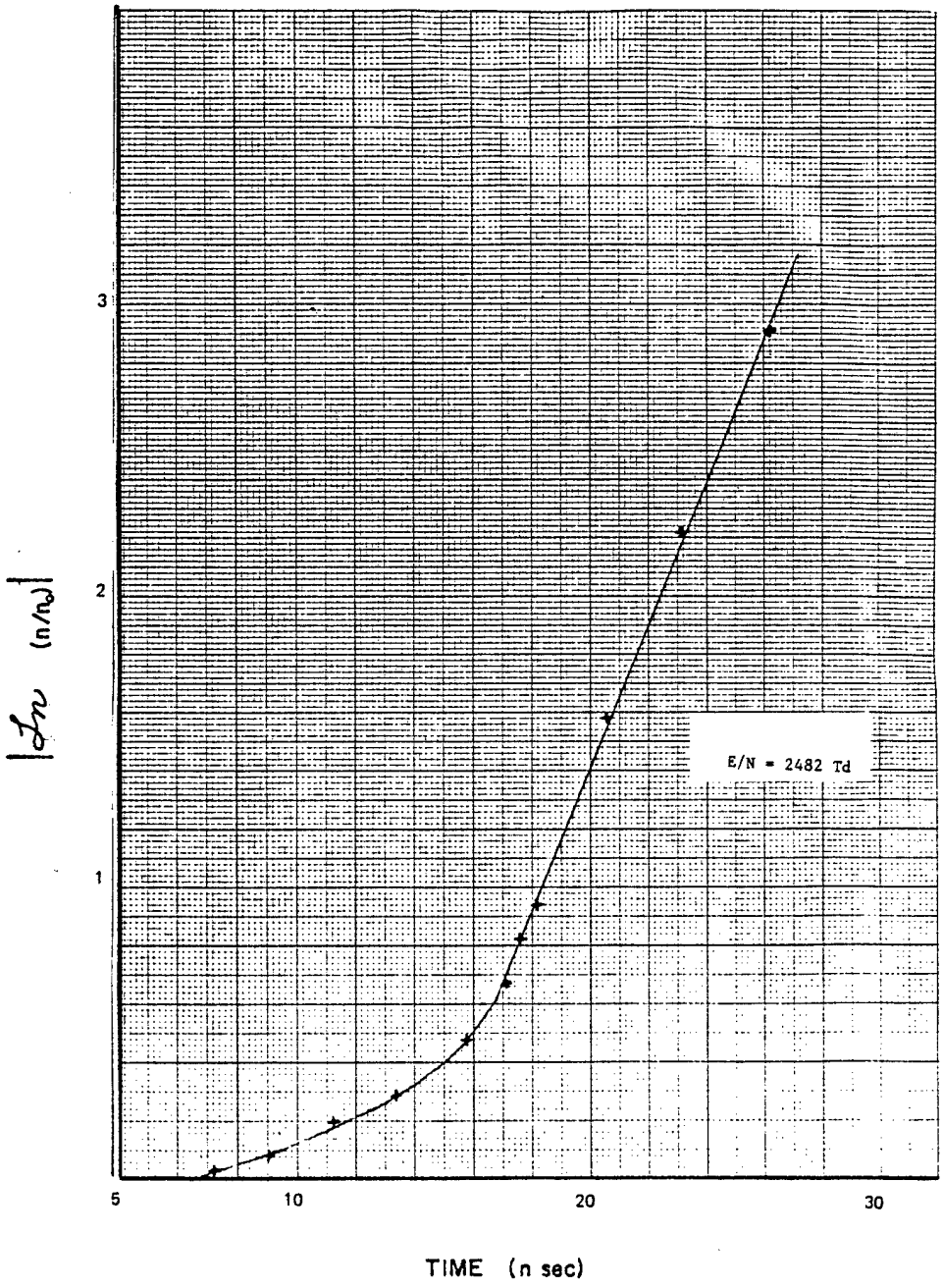

Fig. 10 Breakdown probability

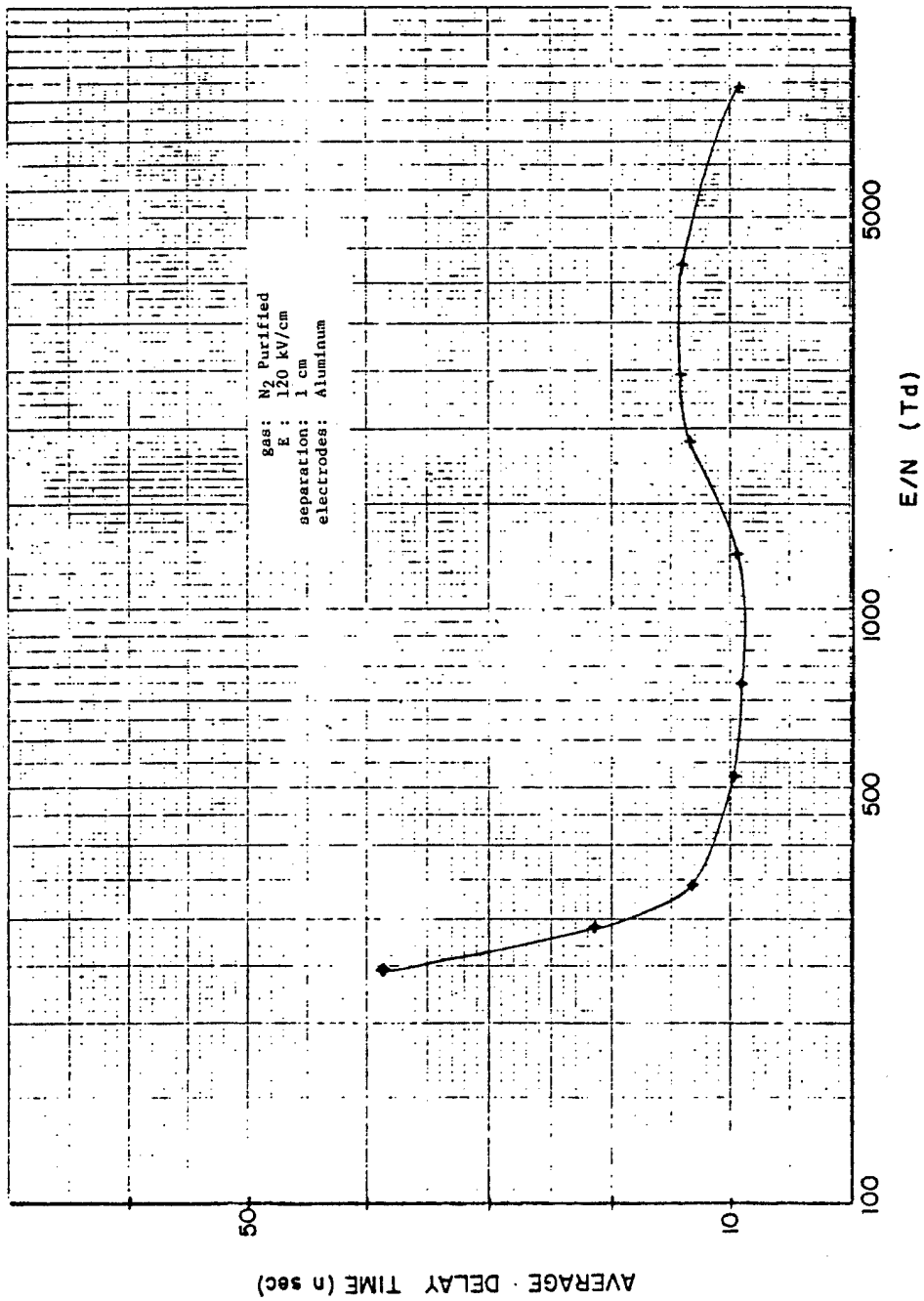

Fig. 11 Average delay time vs E/N

Appendix I.

Review of Gas Breakdown Theories

IEEE TRANSACTIONS ON PLASMA SCIENCE, VOL. PS-8, NO. 3, SEPTEMBER 1

Electrical Breakdown of Gases: The Prebreakdown Stage

E. E. KUNHARDT, MEMBER, IEEE

Abstract—In this paper, a review of the theories and experiments devoted to the understanding of the development of the electrical breakdown of a gas insulated gap, i.e., the switching delay, is presented. The presentation is chronological. The classical Townsend and streamer models for breakdown are discussed; followed by a brief account of the continuous acceleration and avalanche-chain models. These last two models have been proposed primarily to describe breakdown at large electric fields. Then, the two-group model for breakdown at voltages above approximately 20-percent self-breakdown is presented. Finally, a brief analysis is given of the present state of the field and the direction it is taking.

I. Introduction

THE PHYSICS OF HIGH energy densities has recently received a great deal of attention as a common and crucial area of interest for scientists working on high-power lasers, fusion, high-current charged-particle accelerators, and weapons-effect simulators. In the present scenario, the research programs in these areas rely heavily on pulse-power technology to meet their goals. One of the principal problems limiting the further growth of this technology is the development of a switching device that will allow the fast and repetitive transfer of energy from an energy storage device to various transducers (e.g., laser, particle-beam generator, etc.). To meet these diverse requirements [1] a number of novel switching concepts have been proposed. In many of these approaches, switching is accomplished by causing a normally insulating gas to undergo a transition to a conducting state. The various devices that operate in this fashion differ mainly in the way this transition is initiated and in the characteristics of the final conducting stage, i.e., whether it be a glow or arc discharge. The two most popular devices that belong to this category of switches are the thyratron tube and the pressurized spark gap. Presently, these devices are capable of operating in the range of kilovolts and kiloamperes.

In these switching devices, transition from the off to the on state is, in practice, thought of consisting of two phases: 1) the switch delay, i.e., the time elapsed from the desired initiation of the transition to the 10-percent value of the current; and 2) the current rise time, i.e., the 10-percent to 90-percent peak current time. Correlation between these two time intervals and the physical processes occurring in the switch depend on the particular switching device. However, one can say tha general, the delay time is determined by the prebreakdc stage of the insulating gas, whereas the current rise tim determined by a number of factors: the dynamics of the f conducting state, the geometry of the switch, and possi external circuit constraints. In this paper, we would like present a review of the work related to the prebreakdc stage. The purpose is not to compile a catalog of referen but to give an overview of the field and its trend which novice can use as a starting point for further research. T exposition of the material will be presented chronologica This will help the newcomer appreciate the present state understanding, and review for the expert the critical steps the development of the field.

Much of the recent research effort has gone into minimiz the current rise time, and we are now approaching a lir where the total transition time is due mostly to the delay tir The reduction of the switch delay time will require a bet understanding of the physics of the prebreakdown stage. T physics is, to a degree, common to all gas switches, and been very difficult to investigate. This difficulty stems fro first, the broad parameter space traversed by the gas a undergoes breakdown; second, the large number of inter tions taking place in the gas; and third, the fact that all fi variables are inhomogeneous in space. This is further cc pounded by the time scales involved in this progression, i in the nanosecond range in some cases. This requirement speed and the sensitivity constraints imposed on the eqt ment have, until very recently, prevented the experimer investigation of many of the prebreakdown processors. Ne less to say, investigations have concentrated on idealized (fr a practical point of view) situations.

As an illustration of these difficulties, the ionized com nent of the gas first behaves as individual charged parti interacting with a background of neutrals, then as a nonic plasma (i.e., Debye length $\tau_D >$ plasma dimensions) finally as an ideal plasma (i.e., $\tau_D <$ plasma dimensions). single analytical framework can be used to model this tra tion. Moreover, lack of light emission from the very e stages and the short time scale involved has prevented meas ment of the space-time evolution of the electron number sity during this stage.

The text is divided into several sections. In the first sec a standard terminology is established. The subsequent sect form part of one continuous story; however, they have b separated so as to single out major events in the history of field. I conclude with some comments on the present t in the field.

Manuscript received February 5, 1980; revised April 18, 1980. This paper is a summary of a three-day colloquium on prebreakdown processes in gases supported by the Special Applications Branch of the Naval Surface Weapons Center, Dahlgren, VA, under Contract N60921-79C-A187.

The author is with the Ionized Gas Laboratory, Department of Electrical Engineering, Texas Tech University, Lubbock, TX 79409.

0093-3813/80/0900-0130$00.75

II. Statement of the Problem

The physical problem to be discussed is primarily the growth of the ionization of a gas in an electric field and the subsequent breakdown of the insulating properties of the gas (a very comprehensive and up-to-date source of information on this subject is given in [2]).

Two experimental approaches have been used to study this phenomenon. In the first approach [3]-[5] a dc-electric field is applied between two electrodes in a gas (see Fig. 1). The cathode is irradiated with a beam of ultraviolet radiation, generating a constant photoelectric current I_0 at the cathode. For constant values of E/p, where E is the applied electric field and p is the pressure of the gas between the electrodes, measurements of the field intensified current I as a function of electrode separation d are made (Fig. 2). For a given E/p, a separation d_s is reached at which the current becomes self-sustaining. That is, the current I will continue to flow in the circuit even after the external source of ionization has been terminated. This self-sustaining state is called a Townsend discharge [6]. Under these conditions, and if the resistance R allows it, the current will increase indefinitely (i.e., limited by the power supply) and further transitions to a glow and subsequently to an arc discharge will be observed [6]. The duration of the intermediate glow stage depends on a number of parameters (pressure, electrode material, etc.).

In the context of this work, breakdown is defined as the transition from a nonself-sustaining discharge to a Townsend discharge [7]. The voltage across the gap for this transition to occur is called the self-breakdown voltage V_{sb}. Using a similar experimental arrangement, pulse experiments also have been carried out. In these experiments, the magnitude of the applied voltage pulse is less than V_{sb}. The purpose here is to study the space-time evolution of an initial bunch of electrons released at the cathode by a flash of ultraviolet radiation. These experiments are referred to as swarm experiments [2]. Information obtained from both the dc and the pulsed experiments are then used in support of a broader space-time dependent theory (see Section III) and as a tool to measure some of the fundamental parameters associated with this theory.

In the second approach, a coaxial arrangement as shown in Fig. 3 is used [8]-[10]. A voltage pulse of magnitude greater than the static breakdown voltage V_{sb} is launched in the coaxial line and it appears across the electrodes formed by an interruption in the center conductor of the coaxial line. The voltage across the gap or the current in the transmission line is recorded as a function of time. A schematic indication of the evolution of the gap voltage as a function of time is shown in Fig. 4(a) and (b). The time elapsed from the application of the high voltage across the electrodes to the observed time for the collapse of the voltage, across the gap, i.e., T_0 is called the observational time lag and constitutes what in practice is called the switch delay. A second transition to a lower voltage may be observed (i.e., T_a in Fig. 4(a)). This corresponds to the onset of an arc discharge. As the pressure of the gas in the gap and the applied voltage pulse is increased, the interval $T_a - T_0$ becomes shorter in duration. Finally, a situation occurs where only one transition is observed, as shown in Fig. 4(b).

With this technique, it is difficult to correlate the current-voltage measurements made with the physical processes in the gas. In particular, one cannot identify for certain the transition occurring at T_0. At low pressures (i.e., ~100 torr) this transition can be attributed to the breakdown of the gas, i.e., the establishment of a self-sustaining Townsend discharge which almost immediately goes over into a glow discharge with maintaining voltage V_g (see Fig. 4(a)). For these conditions, the observational time lag consists of two portions: the statistical time lag (the time elapsed from the application of the voltage to the appearance of a breakdown initiative electron in the gap), and the formative time lag (the time it takes the space charge to grow in the gap which leads to breakdown). In externally triggered gas switches (laser or electron-beam triggered, for example) the statistical component of the switch delay is practically nonexistent [11], [12]. This type of experiment represents a different regime since the space charge introduced by the triggering mechanism can be very large.

At high pressures (i.e., ~1 atm) and for voltages a few percent above V_s (see Fig. 4(b)), the transition at T_0 cannot, with certainty, be correlated to the breakdown of the gas as we have defined it [13]. This problem has been the topic of considerable debate and will be discussed later in Section IV.

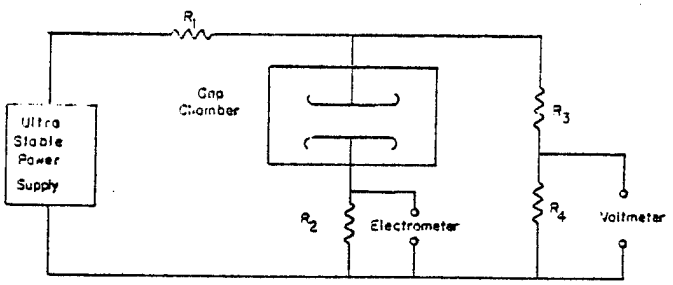

Fig. 1. Diagram of circuit used for the measurement of steady state ionization currents. The gap electrodes are shaped to produce a uniform field in the interelectrode region. The electrode separation is made variable (see [4]).

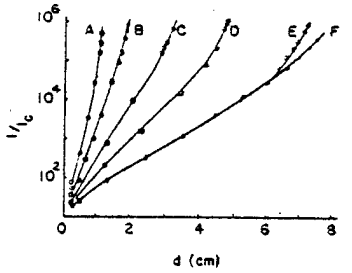

Fig. 2. Log I/I_0 versus gap separation curves taken from J. Dutton, *et al.* [29] showing the exponential growth of the field intensified current.

III. The Townsend Theory of Breakdown

Early work in this field was carried out by Townsend using an experimental arrangement similar to that shown in Fig. 1 [14]. In this work, the current in the external circuit as a function of electrode separation was found to obey the following relationship:

$$I = I_0 \exp(\alpha d) \tag{1}$$

where α is the Townsend primary ionization coefficient. This coefficient corresponds to the number of secondary electrons generated by a primary electron in moving 1 cm along the field

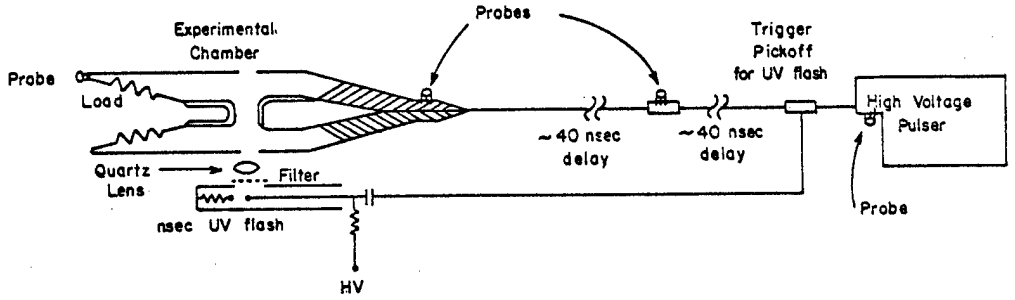

Fig. 3. Schematic diagram of experimental arrangement used in pulsed breakdown experiments.

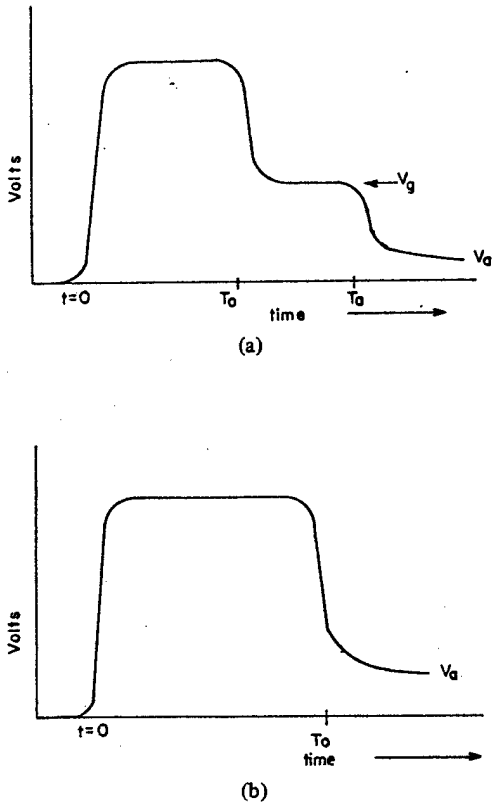

Fig. 4. Schematic indication of the evolution of gap voltage with time. (a) Low pressure. (b) High pressure.

direction. A plot of $\ln (I/I_0)$ versus d is a straight line whose slope is α as shown by the lower portion of the curves in Fig. 2. As the separation d increases, the curves begin to deviate from this straight line indicating that other processes begin to have an influence on the value of the current. To account for this deviation, Townsend proposed that the ions formed by the advancing primary electrons contribute to the growth of the current by creating, as they move towards the cathode, more electron-ion pairs via collisions with the neutrals [14]. A number of other "secondary" processes have since been found which play a larger role in accounting for the faster than exponential growth of the current. A number of these processes have been discussed by Llewlyn Jones [6]. The most important of these secondary processes are ion impact on the cathode and the photoelectric effect at the cathode resulting from the incident flux of photons generated in the gap volume.

Taking these processes into account, the current in the circuit is found to be given by [6]

$$I = \frac{I_0 \exp(\alpha d)}{\left[1 - \frac{\omega}{\alpha}(\exp(\alpha d) - 1)\right]} \tag{2}$$

where ω is a generalized Townsend secondary ionization coefficient, which depends on the various secondary processes present [6]. As shown in Fig. 2, this expression describes the experimental data quite well. As the electrode separation is increased, note that the slope tends toward infinite. At $d = d_s$, the gap breaks down; i.e., I is finite for $I_0 = 0$. The breakdown criterion is obtained from (2) by setting the denominator to zero. This criterion is thus

$$\frac{\omega}{\alpha}(\exp(\alpha d) - 1) = 1. \tag{3}$$

As pointed out by Llewlyn Jones [3], this criterion for breakdown should be taken more as a physical interpretation of the conditions in the gap than as a derived mathematical criterion, since the theory as presented above is a steady state theory which has no provisions for transient events such as breakdown. Thus (3) implies that breakdown occurs when the secondary processes resulting from the motion of a primary electron, and the $\exp(\alpha d)$ electrons it subsequently creates in traversing the gap (i.e., an avalanche), are sufficient to regenerate the primary electron at the cathode. In this context, the current becomes self-sustaining. Under transient conditions, the time it takes for a gap to breakdown depends on the nature of the secondary process. Assuming that ion impact on the cathode is the most important mechanism, the breakdown time becomes inversely proportional to the ion drift speed, i.e., in the microsecond range [6]. Since the processes are statistical, the cumulative effect of a number of avalanches are needed in order to insure that the rejuvenation process of primary electrons will not cease. A number of criteria, similar to (3), for the breakdown of a gap have been obtained [7], [15]. They differ in the functional form of the coefficient ω, which varies in accordance to what is considered to be the most important secondary mechanism.

Since α/p is a unique function of E/p, and further, if one assumes that ω/p is also a function of E/p (this has been experimentally confirmed [3]), then (3) represents a functional relationship between the electrode separation and the

voltage at which breakdown occurs. This fact was first observed experimentally by De la Rue and Muller [16], and was later extensively studied by Paschen [17]. Letting $\alpha/p = f(E/p)$ and $\omega/p = F(E/p)$, (3) can be rewritten as [3]

$$\frac{F(E/p)}{f(E/p)}(\exp(f(E/p)\,pd_s) - 1) = 1. \tag{4}$$

Since $E = V_{sb}/d_s$, the above equation can, after solving for V_{sb}, be rewritten as

$$V_{sb} = \Phi(pd_s) \tag{4a}$$

which means that the breakdown voltage V_{sb} of the uniform field gap is a unique function Φ of the product of pressure and electrode separation for a given gas and electrode material. This relationship is called the Paschen Law.

In certain regimes, the functional relationship between α/p and E/p can be approximated by [18]

$$\alpha/p = A \exp(-Bp/E) \tag{5}$$

where A and B are constants for a given gas. Assuming that ion impact on the cathode is the most important secondary process, $\omega/\alpha \simeq \gamma$, where γ is the probability that a secondary electron will be ejected from the cathode upon impact by an ion [3]. Using (5) and the experimentally observed fact that γ is a slowly varying function of E/p over a wide range, and after solving for V_{sb}, (4) becomes

$$V_{sb} = \frac{Bpd_s}{C + \ln(pd_s)} \tag{6}$$

where

$$C = \ln \frac{A}{\ln\left(\frac{1}{\gamma} + 1\right)}. \tag{6a}$$

From this equation it can be seen (Fig. 5) that at large values of pd_s the breakdown voltage V_{sb} increases with increasing pd_s. Similarly, at low values of pd_s, V_{sb} increases with decreasing pd_s. In the transition from low to large values of pd_s, the breakdown voltage goes through a minimum (the Paschen minimum). This minimum breakdown voltage is obtained from (6) by differentiating with respect to pd_s and equating the result to zero. This gives [19]

$$V_{sb_{min}} = 2.718 \frac{B}{A} \ln\left(1 + \frac{1}{\gamma}\right) \tag{7}$$

and

$$pd_{s_{min}} = \frac{2.718}{A} \ln\left(1 + \frac{1}{\gamma}\right). \tag{8}$$

With a voltage lower than $V_{sb_{min}}$, it is impossible to cause the breakdown of a uniform field gap no matter what the spacing or pressure is.

A number of experimental investigations (of Type I) to confirm Paschen's Law have been carried out [20], [21]. The experimental results agreed quite well with (6) for values of $pd_s \lesssim 200$ mmHg · cm. However, for large values of pd_s, no such agreement was found in these early experiments.

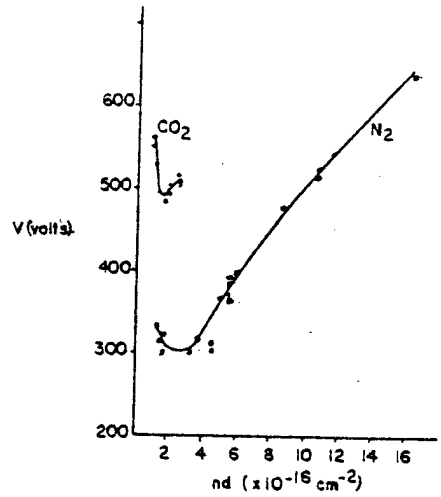

Fig. 5. Comparison of the experimental and calculated values of the static breakdown voltage as a function of gap separation. The curve is taken from [2, p. 228].

At the same time, experiments of Type II were being conducted for large values of pd and overvoltage conditions [22]. Formative times of the order of 10^{-7} s were observed. These values were too small to be associated with the γ process which was considered to be the most important secondary mechanism at the same time. These results and the deviation from Paschen's Law observed at high pressures, gave rise to a number of questions regarding the validity of the Townsend Theory at large values of pd [23], [24]. Three issues were of primary concern. First, the formative time lags in Type II experiments were much shorter than the microsecond time lag predicted from arguments compatible with the Townsend Theory. Second, experiments of Type I, for large values of pd, seemed to indicate that the breakdown potential V_{sb} was, to a very high degree, independent of the cathode material. Third, the breakdown was filamentary in character, which was not consistent with the Townsend Theory of breakdown. A "listing" of the objections to the Townsend Theory as result of the experimental observations available at the time was given by Meek [24]. Additional details on the Townsend Theory can be found in [3], [6], [7].

IV. The Streamer Theory

As a consequence of the above objections to the Townsend Theory, a new theory was proposed, independently, by Meek [24], Raether [22], and Loeb [25]. Meek's objectives were to obtain a modified form of (6) which would be compatible with the experimental observations at high values of pd. The others directed their attention to the observed short time lags and to the filamentary character of the breakdown.

In reality, theirs was more than one theory [26]. However, the fundamental principle used by these investigators in the development of their theory was common to all. This idea was that at a certain stage in the development of a single avalanche, photoionization of the gas in the interelectrode space became

the most important mechanism in determining the breakdown of the gap. The main difference between the theories lay in the stage at which departure from the avalanche-like development occurred. For Meek and Loeb, this occurred when a single avalanche reached the anode, where as for Raether, it occurred when the avalanche was somewhere in the middle of the gap. From this stage on, the theories invoked different physical arguments to explain the breakdown of the gap. However, they all used photoionization of the gas surrounding the avalanche as the principal mechanism.

According to Raether [23], on its way to the anode, the avalanche reaches a critical dimension (determined by the number of electrons in the avalanche or conversely by the space charge field produced by the avalanche) such that secondary electrons begin to be generated just ahead of the avalanche by photoionization of the gas caused by the ionizing radiation generated in the avalanche. Of these electrons, there is a group located just ahead of the avalanche and close to the avalanche axis. This group is in a region of high field due to the enhancement caused by the avalanche space charge. In this region of high α, the electrons can multiply efficiently (1) generating a space charge cloud which rapidly grows to the dimension of the parent cloud, but at a position closer to the anode. The process is repeated continuously to the anode boundary. This progression, due to photoionization, is called a streamer (see Fig. 6). Since the photons generating the secondary electrons propagate at the speed of light, and since the subsequent growth of the space charge is very fast (it occurs in an enhanced field), the propagation time from the parent avalanche to the anode is very small. Once the anode is reached, Raether argues, a similar process begins to occur at the cathode end of the parent avalanche. There the photoelectrons generated are accelerated towards the avalanche extending the ion sheath of the parent avalanche towards the cathode (Fig. 6). Breakdown occurs immediately upon the space charge cloud reaching the cathode.

On the other hand, Loeb and Meek considered only the cathode directed streamer. That is, they assumed that the parent avalanche becomes "critical" just in front of the anode.

What determines the critical stage? Meek arbitrarily chose it to be when the field due to the avalanche is equal to the external field. Using this argument he found that the breakdown equation (i.e., Paschen's Law) becomes [24]

$$(\alpha/p)\,(pd) + \ln\frac{\alpha}{p} = 14.46 + \ln\frac{E}{p} - \frac{1}{2}\ln pd + \ln d. \qquad (9)$$

Raether, on the other hand, defined the critical stage from experimental observations of avalanche development in a cloud chamber. He observed that streamers developed when [23]

$$\alpha X_{cr} \simeq 20$$

where X_{cr} is the average position of the avalanche when it becomes critical. Using this, he calculated a formative time for breakdown. He argued that since the streamer propagation velocity is high (of the order of the speed of light), the formative time is basically the time it takes an avalanche to become critical t_{cr}. This time is given by [23]

$$t_{cr} \simeq \frac{X_{cr}}{V_e} \simeq \frac{20}{\alpha V_e} \qquad (10)$$

where V_e is the electron drift velocity in the applied field. The values obtained from (9) and (10) were very close to experimental observations.

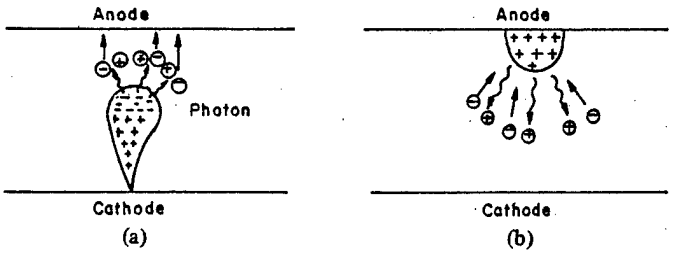

Fig. 6. Sketch of the propagation of a streamer due to gas ionizing radiation. (a) Anode directed streamer. (b) Cathode directed streamer.

Further support for the streamer theory came from Type II experiments by Fletcher [8]. He also tried to improve the mathematical framework of the theory; however, the fundamental premise, i.e., photoionization of the gas was left unquestioned. Similar types of experiments were carried out by Felsenthal and Proud [28]. They were able to explain their results, however, using a modified pulsed-microwave breakdown theory [28]. Further details on the streamer theory may be found in [8], [23]-[25], [28].

V. The Poststreamer Era

In the preceding two sections, the two principal models proposed to explain the initial phase of breakdown were discussed. At low values of pd (i.e., $pd < 200$ mmHg · cm), it was generally agreed that the Townsend Theory gave a satisfactory explanation of the observed phenomena. At the high values of pd, there was no general agreement as to a theory for breakdown [3], [7].

At this time, two schools regarding breakdown at high values of pd developed. One group contended that the Townsend mechanism, which involves the interaction of primary and secondary processes associated with the cathode, was still operative. The other group supported the streamer mechanism. The burden of proof lay with the proponents of the Townsend mechanism since the inconsistencies between the Townsend theory and experiments were still unresolved. The work by this later group concentrated in three areas.

Firstly, experiments of Type I were carried out with increasingly better accuracy by Llewelyn Jones and his colleagues at Swansea [3]-[5]. The purpose of these experiments was to show that the apparent departure from Paschen's Law observed at high pressures was due to poor experimental conditions. Llewelyn Jones argued that, at high pressures, a very stable voltage source was necessary in order to observe the effects of cathode material on the breakdown voltage (i.e., the up curving in Fig. 2). This may be seen from (4). The frac-

tional change in breakdown voltage is given by [3]

$$\frac{\Delta V_{sb}}{V_{sb}} = \frac{\Delta(\omega/\alpha)}{\omega/\alpha} \Big/ \left[V_{sb} f' \left(\frac{V_{sb}}{pd_s} \right) \right]. \tag{11}$$

For large values of pd_s, V_{sb}/pd_s is approximately constant, so that $\Delta V_{sb}/V_{sb} \sim 1/V_{sb}$. It follows that for large V_{sb}, $\Delta V_{sb}/V_s$ can become small enough to be unobserved with the experimental voltage supplies used in earlier experiments. In the last measurements done at Swansea, the effects of secondary processes were observed for pd_s values up to 12 000 mmHg · cm [29].

Secondly, a space/time dependent formulation of breakdown based on the Townsend-type mechanism taking the space charge and the photoelectric effect into consideration was developed. The idea was to show that short breakdown times ($\sim 10^{-7}$ s) could be obtained under a modified Townsend formulation. The first attempt in this direction was by Davidson [30] who obtained an analytic solution for the growth of ionization in the gap assuming that space charge effects were negligible. The inclusion of space charge effects made the solution to the problem analytically untractable: a numerical solution of the system of equations [31] was required. This study showed that short time lags ($\sim 10^{-7}$ s) could indeed be obtained using a Townsend model. Moreover, it was shown by Dickey [13] that even the very short time lags observed by Fletcher [8] ($\sim 10^{-9}$ s) could be explained if the effect of the motion of the space charge in the gap on the external circuit is taken into consideration. He noted that if a large space charge is moving across the gap, a large current can be generated in the external circuit which can (because of the drop in voltage across the external resistance) cause the collapse of the voltage across the gap. Thus a voltage collapse is observed even before the gap is bridged by the space charge. The values he obtained for the time lags using this argument were close to those observed by Fletcher [13]. Thus what constitutes "breakdown" under these conditions is not only different from the definition given earlier, but is difficult to define.

The third area was the issue of interpreting luminosity observations. Raether first noted from luminosity observations that the velocity of propagation of a streamer was of the order of 10^8 cm/s [23]. Subsequently, a number of photographic experiments were carried out which yielded conflicting results as far as the development of the streamer [32]–[34]. In experiments by Wagner [32], the streamer was observed to have two different velocity stages; whereas, experiments by Chalmers [33] showed there is a single propagating velocity. These discrepancies may be due to sensitivity differences in the streak camera or film [34]. However, as was pointed out by Llewelyn Jones [6], luminosity measurements could be very misleading. He disagreed with Raether's conclusions about streamer propagation obtained from the luminosity observations. He suggested that the "streamer" seen by Raether was merely a luminous "phase" effect and that no real physical process was developing in the gap [6]. That is, that the propagation of the luminosity front was due to the temporal growth of the space charge to a level which can be recorded from its luminosity, and not to the spatial propagation of the space charge. Computer simulations subsequently were carried out at Swansea to show that this interpretation was indeed correct [35], [36]. The results seem to agree quite well with an experiment by Wagner [32]. The simulations did not take photoionization into account. A comprehensive compilation of this work is given in [37]. Reference [38] gives a review of luminosity studies.

Since the time lags predicted from the Townsend and streamer theories were different, a discontinuity in the time lag versus pd curve should be observed, indicating the transition from one regime to the other. The first experiment (Type II) designed to look for such transition was carried out by Fischer and Bederson [39]. The results were rather dramatic and completedly changed the traditional boundary separating the two mechanisms. They found that for applied voltages slightly above V_{sb}, long time lags were observed for pd values up to 1000 mmHg · cm. The time lags decreased continuously as a function of the percent overvoltage. This decrease they attributed to the role played by the avalanche space charge and by the photo-electric effect. It was concluded from these experiments that percent overvoltage, and not pd, was the principal parameter determining the value of time lag. This was later confirmed by the computer analysis of Ward [40]. Allen and Phillip [41] later extended these experiments to larger values of percent overvoltage and to a number of different gases. Their results showed a change in the slope of the time lag versus percent overvoltage curve for some of the gases studied. This they interpreted as an indication of a transition from the Townsend regime to the streamer regime.

It should be mentioned that a large amount of work in atomic physics was carried out during this period which helped elucidate the importance of the various processes occurring during breakdown. Moreover, they provided increasingly more accurate values for the various transport coefficients used in the numerical calculations. For more information on this type of experiments the reader should consult [2].

For the streamer group, a number of experiments were carried out to measure the spectrum of the radiation generated by the avalanche and the absorption coefficient for the "ionizing" radiation [43], [44]. During this time, very little was added to the fundamental theories of Raether, Meek, and Loeb, until Lozanskii [15] in 1968 tried to explain the nature of the process for photoionization ahead of the avalanche. This has been an ill-defined issue in the streamer theory and has been questioned by many authors [3], [45]. The main issue has been whether or not photons of high enough energy to photoionize are produced by the avalanche, and if they are produced, can they escape the avalanche? This question is particularly difficult to answer in experiments with relatively pure gases [27]. Lozanskii proposed that associative ionization of atoms excited by photons of energy lower than that required to ionize are responsible for the formation and propagation of the streamer. Assuming a Lorentzian profile for the spectral line of interest, he obtained an expression for the

absorption coefficient of these lower energy photons [15]. Because of the spectral line width, the off resonant photons can escape the avalanche and excite atoms just ahead of the avalanche. He then estimated the number of electrons that will be produced via the chemical reaction

$$A^* + B \rightarrow AB^+ + e^- \tag{12}$$

where A^* is an excited atom or molecule and B is an atom or molecule in the ground state. The cross section for this reaction is rather large. In helium, for example, the cross section for the reaction [27]

$$He^* + He \rightarrow He_2^+ + e^- \tag{13}$$

has a value of $\sim 10^{-15}$ cm^2. The number of electrons produced ahead of an avalanche via this process is sufficient to create and maintain a streamer. However, the occurrence of this (or any other process) has not been confirmed experimentally. Computer simulations for overvolted gaps ($\gtrsim$ 20-percent self-breakdown) have been carried out by Kline [46] and by Yoshida and Tagashira [47]. The absorption coefficient used by Yoshida, *et al.*, for the radiation was consistent with the Lozanskii mechanism. Good agreement was obtained between these simulations and experiments done by Wagner [32] and Koppitz [48] for overvolted gaps. In Koppitz's experiments, the breakdown was large in cross section and thus it was more justifiable to apply the one-dimensional theory used in the computations. The large discharge cross section was achieved by illuminating the cathode surface with ultraviolet radiation. One should recall that success in modeling Wagner's experiment was also achieved without taking photoionization into account [35].

It follows from the works mentioned above that a properly formulated theory (i.e., including space charge and photoelectric effects) based on the Townsend mechanism is able to adequately describe the breakdown processes of a gap for large values of pd, as well as, for applied voltages of a few percent above self-breakdown (up to 20 percent); and that the early objections to the theory were due to experimental "idiosyncrases." Thus the regime of validity of the two models was apparently established: Townsend theory for low overvoltage ($<$20 percent), and streamer theory at high overvoltage ($\gtrsim$ 20 percent).

At very high overvoltages (two to three times self-breakdown), the character of the breakdown once again changes [49]: a broad channel is observed as opposed to a filamentary channel. This has been explained by Babich and Stankevich [50] in terms of runaway electrons which can be produced in the gap at these high fields. Experimental evidence of these runaway electrons exists; however, these results are not time resolved so that it is not known when during the pulsed discharge the runaway electrons were produced [51].

For voltages below those of the above experiments, Mesyats and colleagues [52]-[54] obtained values for the formative time which were not in agreement with those obtained using the streamer model. They noted that the "breakdown time" depended on the number of initiating electrons at the cathode. For large numbers of initiatory electrons ($\sim 10^4$), Mesyats derived an expression for the "breakdown time" using arguments similar to Dickey's [53]. He pointed out that this was indeed the initial condition in Fletcher's experiment. For low number of initiatory electrons (which he called single electron initiation), the "breakdown time" was long compared to that obtained from the streamer model [54]. He argued that since the time for an avalanche to become critical, at these high values of electric field, was much shorter than the average lifetime of the excited atoms, photoionization played no role in the breakdown process; moreover, that the avalanche stops growing due to the decrease in field at the avalanche head due to the local space charge. At this point, a new avalanche develops ahead of the parent avalanche which goes through the same cycle. Thus an avalanche chain is formed which slowly drifts across the gap. He called this the avalanche chain model, where a linear chain of avalanches, originating at the cathode and supported by the photoelectric effect at the cathode, is responsible for bridging the gap [54].

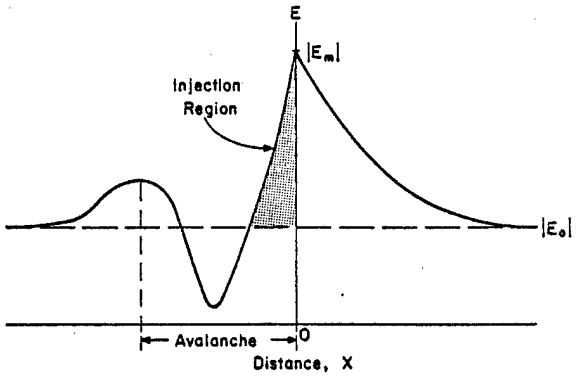

Fig. 7. Schematic indication of axial electric field in avalanche region [55].

The present state of affairs is that the domain of overvoltage is divided as follows: Townsend model, streamer model, avalanche chain model, and the continuous acceleration model.

Recently, Kunhardt and Byszewski [55] introduced a model for the development of breakdown above the Townsend regime. The model offers the attractive feature of the unification of all the proposed breakdown phenomena. That is, it gives a continuous picture of the breakdown above the Townsend regime, and merges into the Townsend avalanche picture as the voltage is reduced.

In this model, the energy distribution function for electrons in the advancing avalanche is assumed to have two components: fast electrons and slow (thermal) electrons. The fast electrons can "run away" from the avalanche. This happens because the effective retarding force on an electron moving through a neutral gas decreases with increasing velocity, in the case of electrons possessing sufficiently high energy (i.e., $u \gtrsim 3\text{-}5\epsilon_i$, where ϵ_i is the ionization energy). The energy threshold for these runaway electrons is determined by the electric field strength (Fig. 7(a)) and the gap parameters. Once these fast electrons leave the avalanche, most of them no longer meet the runaway condition and become "trapped." This is due to the fact that they enter a region of decreasing field ahead of the avalanche, and the energy they gain from the field along their trajectory is not enough to overcome the losses (Fig. 8). The "trapping" distance of these electrons is a

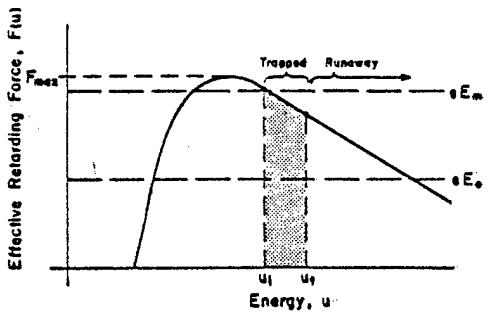

Fig. 8. Retarding force versus electron energy [55].

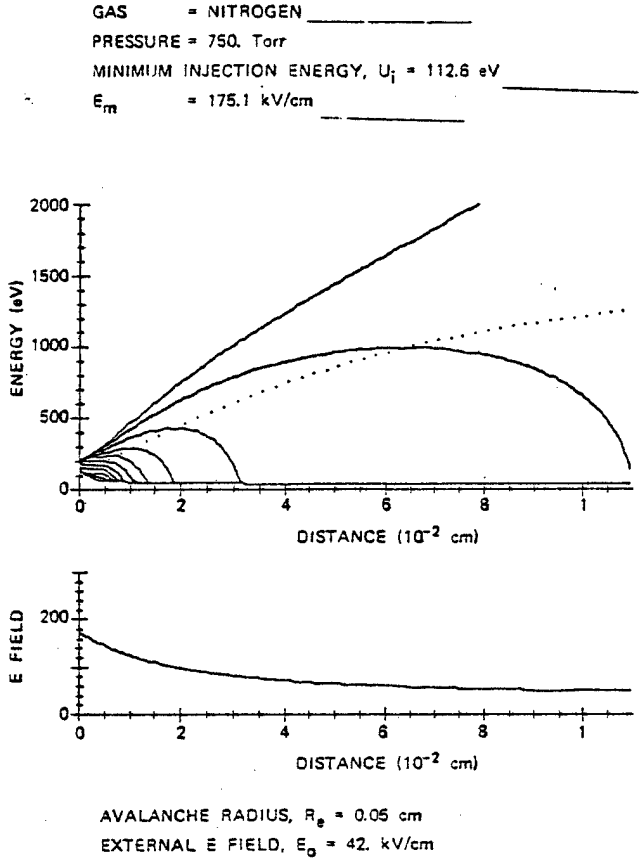

Fig. 9. Electron energy versus distance from avalanche front [55].

function of their initial energy (Fig. 9). Thus these "seed" electrons, which are continuously "emitted" from the avalanche, multiply at various distances from the parent avalanche rapidly extending the avalanche space charge towards the anode. On the cathode side, the photoelectric effect is assumed to be the primary mechanism for generating secondary electrons which are subsequently accelerated towards the high field region of the parent avalanche.

This model has been used to explain, among other things, the variations in the time lag versus percent overvoltage observed by Allen and Phillips [41] for different gases, and the "broad" breakdown observed by Koppitz [48] when the initial ultraviolet irradiation covered a large portion of the cathode surface.

The most important concept associated with an avalanche is that of the nature of the electron distribution function [56]. At present, this is one of the principal areas of investigation [57]-[60]. Because of the complexity of the problem, the work is mainly computational, although some analytical attempts have been made [61]. Computationally, Monte Carlo [57], [58] and Boltzman [59], [60] codes with varying degrees of sophistication have been used. The thrust is to arrive at the distribution function for electrons in regions of high electric fields and large spatial gradients. No model can conclusively be validated until this distribution is obtained.

Our ability to manipulate the switch delay time will depend on our understanding of the evolution of the electron energy distribution function under these highly "nonequilibrium" conditions.

Acknowledgment

I would like to express my appreciation to Dr. A. H. Guenther for reading the manuscript and making a number of valuable suggestions.

References

[1] T. R. Burkes, "A critical analysis and assessment of high power switches," Naval Surface Weapons Center Rep. NP30/78, Sept. 1978.
[2] J. M. Meek and J. D. Craggs, Eds., *Electrical Breakdown of Gases*. New York: Wiley, 1978.
[3] F. Llewellyn Jones, "Ionization growth and breakdown," *Hand. Phys.*, vol. 22, pp. 1-92, 1956.
[4] W. E. V. J. Davies, J. Dutton, and F. M. Harris, "An apparatus for the investigation of pre-breakdown ionization in gases at high voltages, high gas pressures and large electrode separations," *J. Sci. Instrum.*, vol. 43, pp. 457-461, July 1966.
[5] J. Dutton, F. Llewellyn Jones, and W. R. Palmer, "Electrical breakdown of gases: Ionization growth in air at high pressures," *Proc. Phys. Soc.*, vol. 78, pp. 569-583, Oct. 1961.
[6] F. Llewellyn Jones, *Ionization and Breakdown in Gases*. London, England: Methuen, 1966.
[7] L. B. Loeb, "Electrical breakdown of gases with steady or direct current impulse potentials," *Hand. Phys.*, vol. 22, pp. 445-530, 1956.
[8] R. C. Fletcher, "Impulse breakdown in the 10^{-9} sec range of air at atmospheric pressure," *Phys. Rev.*, vol. 76, pp. 1501-1511, Aug. 1949.
[9] V. E. Nesterikhin, V. S. Komel'Kov, and E. Z. Meilikhov, "Pulsed breakdown of small gaps in the nanosecond range," *Sov. Phys.-Tech. Phys.*, vol. 9, pp. 40-52, July 1964.
[10] A. Doran and J. Meyer, "Photographic and oscillographic investigations of spark discharges in hydrogen," *Brit. J. Appl. Phys.*, vol. 18, pp. 793-799, Mar. 1967.
[11] A. H. Guenther and J. R. Bettis, "The laser triggering of high-voltage switches," *J. Phys. D: Appl. Phys.*, vol. 11, pp. 1577-1613, June 1967.
[12] K. McDonald, M. Newton, E. Kunhardt, M. Kristiansen, and A. H. Guenther, "An electron-beam triggered spark gap," this issue. pp. 181-185.
[13] F. R. Dickey, Jr., "Contribution to the theory of impulse breakdown," *J. Appl. Phys.*, vol. 23, pp. 1336-1339, Dec. 1952.
[14] J. S. Townsend, *The Theory of Ionization of Gases by Collision*. London, England: Constable, 1910.
[15] E. D. Lozanskii, "Photoionizing radiation in the streamer breakdown of a gas," *Sov. Phys.-Tech. Phys.*, vol. 13, pp. 1269-1272, Mar. 1969.
[16] W. de LaRue and H. W. Muller, "Experimental researches in the electric discharge with the chloride of silver battery," *Phil. Trans. Roy. Soc. London*, vol. 171, pp. 65-116, Jan. 1880.
[17] F. Paschen, *Wied. Am.*, vol. 37, pp. 69, 1889.
[18] A. H. Von Engel, "Ionization in gases by electrons in electric fields," *Hand. Phys.*, vol. 21, pp. 504-573, 1956.
[19] —, *Ionized Gases*. London, England: Oxford, 1955.
[20] W. R. Carr, "On the law governing electric discharge in gases at low pressures," *Phil. Trans. Roy. Soc. London*, vol. A201, pp. 403-433, May 1903.

[21] F. Llewllyn Jones and A. Henderson, "The influence of the cathode in the sparking potential of hydrogen," *Phil. Mag.*, vol. 28, pp. 185–191, Aug. 1939.
[22] W. Rogowski, "Impulse potential and breakdown in gases," *Arch. Electrotech.*, vol. 20, pp. 99, 1928.
[23] H. Raether, *Electron Avalanches and Breakdown in Gases.* London, England: Butterworth, 1964.
[24] J. M. Meek, "A theory of spark discharge," *Phys. Rev.*, vol. 57, pp. 722–730, Mar. 1940.
[25] L. B. Loeb, *Fundamental Processes of Electrical Discharges in Gases.* New York: Wiley, 1939.
[26] G. M. Petropoulos, "Avalanche transformation during breakdown in uniform fields," *Phys. Rev.*, vol. 78, pp. 250–253, May 1950.
[27] E. D. Lozanskii, "Development of electron avalanches and streamers," *Sov. Phys.-Usp.*, vol. 18, pp. 893–908, Jan. 1976.
[28] P. Felsenthal and J. M. Proud, "Nanosecond-pulse breakdown in gases," *Phys. Rev.*, vol. 139, pp. A1796–A1804, Sept. 1965.
[29] J. Dutton and W. T. Morris, "The mechanism of electrical breakdown of air in uniform fields at voltages up to 400 KV," *Brit. J. Appl. Phys.*, vol. 18, pp. 1115–1120, May 1967.
[30] P. M. Davidson, "Formative time lags in the electrical breakdown of gases," *Brit. J. Appl. Phys.*, vol. 4, pp. 170–175, June 1953.
[31] A. J. Davies, C. J. Evans, and F. Llewellyn Jones," Electrical breakdown of gases: The spatio-temporal growth of ionization in fields distorted by space charge," *Proc. Roy. Soc.*, vol. A281, pp. 164–183, Jan. 1964.
[32] K. H. Wagner, "Die entwicklung der elektronenlawine in den plasmakanal, untersucht mit bildverstärker und wischverschlub.," *Z. Phys.*, vol. 189, pp. 465–515, Feb. 1966.
[33] I. D. Chalmers, H. Duffy, and D. Tedford, "The mechanism of spark breakdown in nitrogen, oxygen, and sulphur hexafluoride," *Proc. Roy. Soc.*, vol. A329, pp. 171–191, Aug. 1972.
[34] M. Bayle, P. Bayle, and M. Crokaert, "The development of breakdown in a homogeneous field at high overvoltages in helium-neon mixtures and nitrogen," *J. Phys. D: Appl. Phys.*, vol. 8, pp. 2181–2189, Oct. 1975.
[35] A. J. Davies, C. J. Evans, P. Townsend, and P. M. Woodison, "Computation of axial and radial development of discharges between plane parallel electrodes," *Proc. Inst. Elec. Eng.*, vol. 124, pp. 179–182, Feb. 1977.
[36] A. J. Davies, C. S. Davies, C. J. Evans, "Computer simulation of rapidly developing gaseous discharges," *Proc. Inst. Elec. Eng.*, vol. 118, pp. 816–824, June 1971.
[37] A. J. Davies and C. J. Evans, "The theory of ionization growth in gases under pulsed and static fields, in *CERN Rep. 73-10*, Geneva, Sept. 1973.
[38] S. C. Haydon, "Spark channels," in *Eighth Int. Conf. Phenomena in Ionized Gases*, Vienna, 1967.
[39] L. H. Fisher and B. Bederson, "Formative time lags of spark breakdown in air in uniform fields at low overvoltages," *Phys. Rev.*, vol. 81, pp. 109–111, Jan. 1951.
[40] A. L. Ward, "Calculations of electrical breakdown in air at near-atmospheric pressure," *Phys. Rev.*, vol. 138, pp. A1357–A1362, May 1965.
[41] K. R. Allen and K. Phillips, "Correlation of the formative time lags with the light emitted from spark discharges," *Proc. Roy. Soc., Ser. A*, vol. 278, pp. 188–213, Jan. 1964.
[42] *Handbuch der Physic.* Berlin, West Germany: Springer, vol. 21–22, 1956.
[43] G. R. Bainbridge and W. A. Prouse, "The absorption of ultraviolet ionizing radiation in gases," *Can. J. Phys.*, vol. 34, pp. 1038–1045, Aug. 1956.
[44] G. W. Penney and G. T. Hummert, "Photoionization measurements in air, oxygen, and nitrogen," *J. Appl. Phys.*, vol. 41, pp. 572–577, Feb. 1970.
[45] J. Dutton, S. C. Haydon, and F. Llewellyn Jones, "Photoionization and the electric breakdown of gases," *Proc. Roy. Soc., Ser. A*, vol. 218, pp. 206–223, Aug. 1953.
[46] L. E. Kline, "Calculations of discharge initiation in overvolted parallel-plane gaps," *J. Appl. Phys.*, vol. 45, pp. 2046–2054, May 1974.
[47] K. Yoshida and H. Tagashira, "Computer simulation of a nitrogen discharge at high overvoltages," *J. Phys. D.: Appl. Phys.*, vol. 9, pp. 491–505, Feb. 1976.
[48] J. Kopptiz, "Nitrogen discharges of large cross-section at high overvoltages in a homogeneous field," *J. Phys. D.: Appl. Phys.*, vol. 6, pp. 1494–1502, July 1973.
[49] Y. L. Stankevich and V. G. Kalinin, "Fast electrons and x-ray radiation during the initial stage of growth of a pulsed spark discharge in air," *Sov. Phys.-Dokl.*, vol. 12, pp. 1042–1043, May 1968.
[50] L. P. Babich and Y. L. Stankevich, "Transition from streamers to continuous electron acceleration," *Sov. Phys.-Tech. Phys.*, vol. 17, pp. 1333–1336, Feb. 1973.
[51] L. V. Tarasova, L. N. Khudyakova, T. V. Loiko, and V. A. Tsukerman, "Fast electrons and x-rays from nanosecond gas discharges at 0.1–760 Torr," *Sov. Phys.-Tech. Phys.*, vol. 19, pp. 351–353, Sept. 1974.
[52] G. A. Mesyats, Y. I. Bychdov, and V. V. Kremner, "Pulsed nanosecond electric discharges in gases," *Sov. Phys.-Usp.*, vol. 15, pp. 282–297, Nov. 1972.
[53] G. A. Mesyats, Y. I. Bychkov, and A. I. Iskol'dskir, "Nanosecond formation time of discharges in short air gaps," *Sov. Phys.-Tech. Phys.*, vol. 13, pp. 1051–1055, Feb. 1969.
[54] V. V. Kremnev and G. A. Mesyats, "Growth of a nanosecond pulsed discharge in a gas with one-electron initiation," *Zh. Prikl. Mekh. Tekh. Fiz.*, vol. 1, pp. 40–45, Jan. 1971.
[55] E. E. Kunhardt and W. W. Byszewski, "Development of overvoltage breakdown in high pressure gases," *Phys. Rev. A.*, vol. 21, pp. 2069–2077, June 1980.
[56] W. P. Allis, "Motions of ions and electrons," *Hand. Phys.*, vol. 21, pp. 383–444, 1956.
[57] Y. Sakai, H. Tagashira, and S. Sakamoto, "The development of electron avalanches in argon at high E/N values: I. Monte Carlo simulation," *J. Phys. D.: Appl. Phys.*, vol. 10, pp. 1035–1049, Mar. 1977.
[58] R. W. L. Thomas and W. R. L. Thomas, "Monte Carlo simulation of electrical discharges in gases," *J. Phys. B., Ser. 2*, vol. 2, pp. 562–570, Jan. 1969.
[59] T. Makabe and T. Mori, "Electron swarm having an anisotropic velocity distribution function," *J. Phys.*, vol. 40, pp. C7-43–C7-44, June 1979.
[60] T. N. An, E. Marode, G. Fournier, and P. Segur, "Electron distribution function in a very non-uniform electric field," *J. Phys.*, vol. 40, pp. C7-533–C7-534, June 1979.
[61] J. L. A. Francey and D. A. Jones, "Analytic solutions to the Boltzmann equation for electrons swarms," *J. Phys. D.: Appl. Phys.*, vol. 9, pp. 457–464, Mar. 1976.

Appendix II

Model that describes the Development of Overvoltage Breakdown

PHYSICAL REVIEW A VOLUME 21, NUMBER 6 JUNE 1980

Development of overvoltage breakdown at high gas pressure

E. E. Kunhardt and W. W. Byszewski
Ionized Gas Laboratory, Texas Tech University, Lubbock, Texas 79409
(Received 22 October 1979)

A model for the development of electrical breakdown in dense gases is presented. It describes the initial phase of breakdown in the regime where the Townsend avalanche mechanism does not apply. The main features of the model are as follows: (1) It gives a continuous picture of the development both in the structure of the breakdown and the physics of the processes, and (2) it is based on electron kinetics, so that the theory is general in scope. In light of this model a brief discussion of experimental results is given.

I. INTRODUCTION

Two basic models have been proposed to explain the initial phase of electrical breakdown in gases at high pressures. These are commonly known as the Townsend avalanche model[1] and the streamer model.[2] The mechanism playing a role in the first model involves the interaction of primary and secondary processes of which cathode processes are generally found to predominate in uniform fields.[3] Photoionization of the gas in the interelectrode volume forms the basis for the second model.[2] Over the last 30 years, considerable effort has gone into establishing the regime of validity of both models. Experimental evidence was sought for the transition between the two regimes, such as an abrupt decrease in the formative time of the breakdown as the voltage was increased above but near the self-breakdown voltage. The results were not conclusive.[4]

The Townsend avalanche model was initially thought to apply only at low pressures and for voltages near self-breakdown. This regime, however, has recently been expanded by the experimental and theoretical works at Swansea[5,6] and by the computer simulations of Ward,[7] to include the high-pressure, small overvoltage regime ($\lesssim 20\%$). This was the regime for which the streamer model was originally proposed. Unlike the Townsend avalanche theory, the foundations of the streamer theory have been very vague from the start.[1] It is important to note that the "streamer model" is actually more than one model, each based on different hypotheses.[8] The clearest physical picture of the processes associated with a streamer model has been given by Lozanskii,[9] who proposed that associative ionization of atoms excited by photons of lower energy than those required to ionize, are responsible for the formation and propagation of the streamer. The initial support for the streamer model came from experiments by Rogowski[10] and Raether,[2] and later by Fletcher,[11] who measured values for the formation time somewhat in agreement with those obtained theoretically. Luminosity measurements initially used by many workers as further evidence in support of the theory, have been shown, in certain cases, to be very misleading.[12] Moreover, as pointed out by Mesyats,[13] agreement in the value of the formative time and, we may add, in the structure of the breakdown process, is a necessary but not a sufficient criterion for the validity of the theoretical premises. Agreement in the formation time was also obtained by Dickey,[14] although his theory was based on a completely different hypothesis.

At very high overvoltages (two to three times self-breakdown voltage), Stankevich and Kalinin[15] have observed that the structure of the breakdown, once again, changes; i.e., a broad channel breakdown is observed as opposed to a filamentary channel. This has been explained by Babich and Stankevich[16] in terms of runaway electrons from the main avalanche. We must point out that there are a few inconsistencies in the paper of Babich *et al.* regarding the criterion for the existence of these runaway electrons. Experimental evidence of these runaway electrons exists.[17] These experiments, however, were not time resolved so that it is not known when during the breakdown runaway electrons were produced.

At voltages below this regime, Mesyats[18] obtained values for the formative time which were not in agreement with those obtained using the streamer model. He then proposed the avalanche chain model, where a chain of avalanches originating at the cathode and supported by the photoelectric effect at the cathode is responsible for bridging the gap.

Thus, at present, the streamer model is thought to qualitatively describe the breakdown processes at high pressures and overvoltages (above 20% self-breakdown), but below Mesyats' avalanche chain regime.

In this paper, we present a model to describe the breakdown processes for all voltages and pressures above the Townsend avalanche domain. We call it the

two-group model due to the similarity between this problem and the neutron transport problem in nuclear reactor physics. It is based on electron kinetics, and it is thus applicable to a broad range of conditions (breakdown in pure gases, for example). The model offers the attractive feature of the unification of all the proposed breakdown phenomena; that is, it provides a continuous picture of the development of the initial phase of breakdown above the Townsend regime both in the structure of the breakdown and the physics of the processes. It merges into the Townsend avalanche picture as the voltage is reduced.

In Sec. II, we will present the model, devoting our attention to the physical processes that occur and that lead to the formation of breakdown. We then proceed, in Sec. III, to attempt to formulate a mathematical framework for the theory. In Sec. IV, we discuss some experimental results in light of the theory presented.

II. TWO-GROUP MODEL OF BREAKDOWN

We will develop a physical picture of the electrical breakdown of a gas at high pressures and for voltages so that the effects of the produced space charge cannot be neglected. This regime lies above the Townsend avalanche regime. It is our purpose in this section to give a clear physical picture of the processes responsible for increasing the propagation speed of the avalanche towards the anode and for causing the filamentary appearance of the evolving avalanche.

Our model is based on electron kinetics rather than photon induced processes. Electrons with a broad spectrum of energies are always present in an avalanche. On the other hand, the existence of photons with enough energy and range to photoionize the gas outside the avalanche has always been a questionable matter, especially in relatively pure gases.[9] The possibility of multiphoton ionization would require photon fluxes not available in the avalanche stage.

A sketch of the experimental situation we want to consider is shown in Fig. 1. Also shown is an avalanche propagating towards the anode. The shape of the avalanche is indicative of the processes at play in the development up to its present location in the gap. The avalanche is divided into three stages (see Fig. 1). This division is strictly for illustrative purposes, since a continuous transformation is actually taking place. In stage I, the radial dimensions of the avalanche is determined primarily by diffusion processes. The avalanche radius is given by[1]

$$r_d = (6Dt)^{1/2}, \tag{1}$$

where D is the electron diffusion coefficient. In

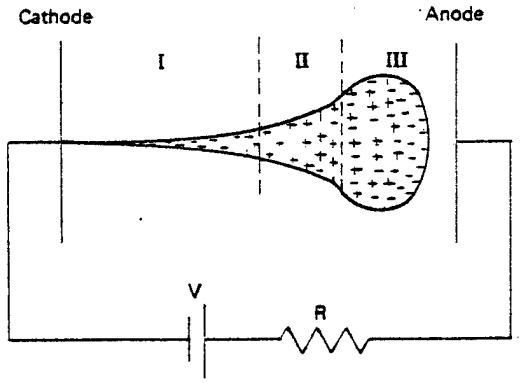

FIG. 1. Sketch of the developed avalanche in the cathode-anode volume.

the regime of interest (i.e., for voltages >20% self-breakdown), the time of development is very short so that very little expansion occurs. We can estimate the value of the radius for the case of breakdown in nitrogen, at atmospheric pressure. Here, $D \simeq 862$ cm^2/sec, $t \sim 10^{-8}$ sec, and from (1), $r_d \sim 7.2 \times 10^{-3}$ cm.

As the number of electrons in the avalanche increases, electrostatic repulsion begins to play a role in the expansion of the avalanche. In this regime (stage II), the avalanche radius increases exponentially with time. This radius may be estimated using the expression[19]

$$r_e = \left(\frac{3e}{4\pi\epsilon_0 E_0}\right)^{1/3} e^{\alpha z/3}, \tag{2}$$

where e is the electron charge, E_0 is the external field, α is the Townsend primary ionization coefficient, z is the average position along the gap axis of the avalanche with $z = 0$ being the cathode position, and ϵ_0 is the permittivity of free space. For breakdown in nitrogen at 1 atm and an applied field of 40 kV/cm (i.e., ~25% above self-breakdown), for which $\alpha \sim 56$ cm^{-1}, the radius of the avalanche at $z = 0.05$ cm is $r_e = 0.14$ cm. The radial expansion is somewhat slowed down in stage III as space-charge neutralization begins to take place.

Throughout these three stages, as the electron and ion densities in the avalanche increase, two things are happening: First, a highly nonequilibrium electron energy distribution is evolving[20] and second, the external field is becoming distorted due to the presence of the space charge. It is the combination of these two effects that play the major role in the following stage, i.e., stage IV. A qualitative picture of the longitudinal field at the axis of the avalanche as a function of distance and just prior to the time the avalanche "enters" into stage IV is given in Fig. 2. The $x = 0$ plane corresponds to the front of the avalanche.

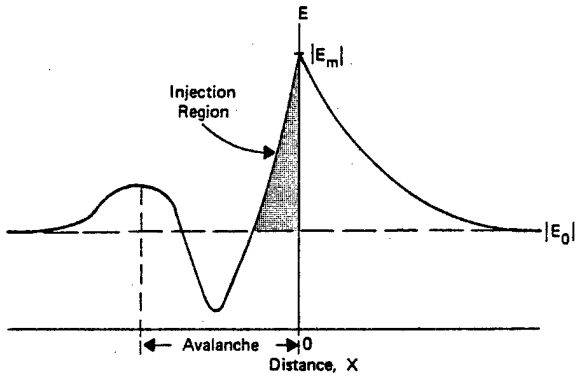

FIG. 2. Sketch of the magnitude of the longitudinal electric field along the axis of the avalanche.

Here, the field attains the maximum average value it can have in the gap E_m, and it decreases away from this plane. The rate of decrease is slower for $x>0$.

The electron energy distribution in the avalanche is far from equilibrium. It is enriched with high-energy electrons, a consequence of the large electric field. Furthermore, it is anisotropic in the high-energy region; it acquires a directed character along the field (this will be further discussed). For the purpose of discussion, we may think of the electron energy distribution as being formed of two groups of electrons: the "main" electron distribution and the "fast" electrons.

It is possible for some of these fact electrons to become runaways, that is, they may continuously gain energy from the field. This happens because the effective retarding force on an electron moving through a neutral gas decreases with increasing velocity, in the case of electrons possessing a sufficiently high energy (i.e., $u \gtrsim 3-5\epsilon_i$, where ϵ_i is the ionization energy). The energy threshold for electron runaway is determined by the magnitude of the electric field. The larger the field, the lower the threshold energy and consequently the larger number of electrons can run away.

In Fig. 2, the region where electrons are most likely to run away is labeled the "injection region." In this region of high electric field, the runaway threshold energy is the lowest and is determined by the maximum field intensity E_m. Since the distribution is anisotropic in this energy regime, the runaway electrons are accelerated out of this region and are injected into the region ahead of the avalanche where the field is decreasing. The number of particles injected is maximum at the axis. Here, the space-charge fields and the external field are colinear, thus giving the maximum total field, hence, the lowest injection energy. As we move away from the axis, the space-charge field and the external field are no longer collinear,

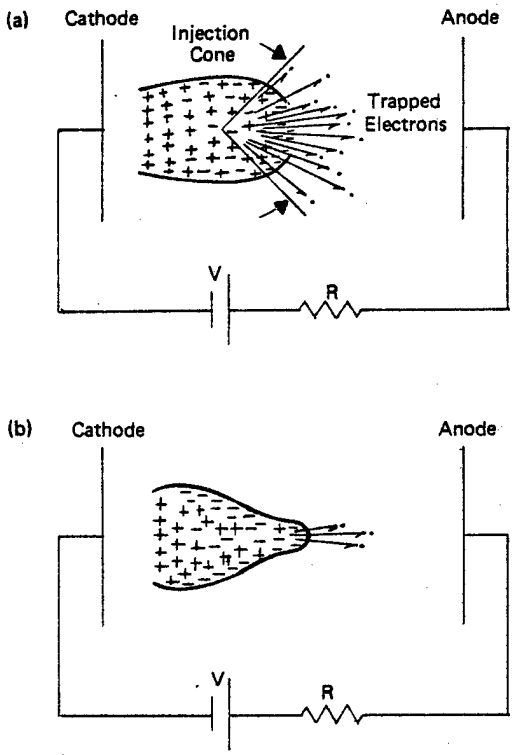

FIG. 3. Development of a filamentary channel ahead of the avalanche.

so that the total field is reduced, thus increasing the runaway threshold energy. We thus observe that there is an injection cone with a maximum on the axis [see Fig. 3(a)].

Once injected, most of the fast electrons no longer meet the runaway conditions and become "trapped"; that is, the energy they gain along their trajectory is not enough to overcome the losses (see Sec. III). The trapping distance (i.e., the distance from the avalanche front to where they become trapped) is for a given gas a function of the initial injection energy of the electrons and the slope of the electric field ahead of the avalanche.

Thus, just prior to stage IV, we may think of the avalanche as a localized distribution of electrons. The beginning of stage IV [Fig. 3(a)] is marked by the "burst" of the avalanche along its axis, followed by the ejection of high-velocity, electrons and their subsequent capture at varying distance from the original avalanche position where they start to generate avalanches of their own.

The captured electrons ionize the gas extending the boundary of the main avalanche along a filamentary channel centered at the axis of the avalanche [see Fig. 3(b)]. Once the channel starts to narrow, the electrical field just ahead of the tip increases. Fast electrons are continuously injected into the region ahead of the tip and again

are trapped. This process accelerates the development of the avalanche tip towards the anode. This was shown by Raether,[2] although his explanation was based on the electrons being produced by photoionization ahead of the avalanche rather than by captured runaway electrons. Thus a filamentary channel (note that the channel is maintained narrow due to the injection cone phenomenon) evolves from the main avalanche whose structure is similar to the classical streamer, although the physics of its formation and subsequent development is quite different. It is possible that for certain gas mixtures, photoionization may be present; however, the electron kinetic effects we have described still play the fundamental role.

Once the avalanche front makes contact with the anode, the field in the cathode side of the avalanche is greatly enhanced. This happens because a conducting path now exists between the cathode tip of the avalanche and the anode. Moreover, the field lines converge toward this tip, so that subsequent avalanches emerging from the cathode can complete the final bridging of the gap.

As the applied voltage increases, two things happen: The avalanche "bursts" closer to the cathode, and the number of untrapped runaway electrons increases. These runaways have been experimentally observed for voltages two to three times the self-breakdown voltage.[17]

III. MATHEMATICAL FOUNDATIONS OF THE TWO-GROUP MODEL

From the discussion in Sec. II it is evident that the breakdown of a gas at higher overvoltages (i.e., $V > 20\%$ self-breakdown) is governed by electron kinetics in a highly inhomogeneous, three dimensional field. A full treatment of the problem would require a knowledge of the space-time-dependent electron energy distribution function and of the space-charge fields in the region bounded by the electrodes, subject to the boundary conditions defined by the secondary processes occurring at the electrodes and by the external supply circuit. This problem is indeed formidable, and the only possibility of it being solved is via computer analysis. In this paper we will not give either an analytical or a computational description of the physics presented in Sec. II; however, we will give a mathematical justification of the hypothesis presented.

Our point of departure is the state of the avalanche just prior to stage IV (see Sec. II and Fig. 1). At this point, we have a weakly ionized medium (typical values for the density of electrons are 10^{11}–10^{12} particles/cm^3) in the presence of an external electric field. From Gurevich's work[20] we say that the electron energy distribution function can be thought of as being formed of two groups: the main distribution electrons and the fast electrons. This discontinuity is again of a mathematical nature to make the problem tractable.

Although the conditions existing during breakdown are transient in character and bounded in space, we will assume that the fast electron distribution just prior to stage IV is, to zeroth order, given by the quasistatic distribution obtained by Gurevich[20] for the case of a weakly ionized plasma in an infinite domain; that is,

$$f_f(v, t) \simeq f(v_0, t) \exp\left[-\frac{2m}{\epsilon_i}\int_{v_0}^{v} v\,dv\left(1-\frac{eE}{F(v)}\right)\right], \qquad (3)$$

where v_0 is the lower boundary of the fast electron distribution, $v_0 \simeq (5\epsilon_i/m)^{1/2}$; ϵ_i is the ionization energy; $F(v)$ is the effective retarding force on an electron moving with a velocity v in a neutral gas; and $f(v_0, t)$ is the main distribution evaluated at $v = v_0$ (and it may be taken as Maxwellian). The fast electron distribution if valid for $v > v_0$.

Instead of the analytical expression used by Gurevich[20] for the retarding force $F(v)$ (see Ref. 21 for further discussion of this retarding force), we retain the same functional dependence on v and introduce two parameters A and B which are then determined from experimental data.[22] The reason for this is that there is a disagreement between the values obtained experimentally and analytically for the position and height of the maximum of the retarding force. Thus, we take $F(v)$ to be

$$F(v) = A'p \ln(v^2/B')/v^2,$$

or letting $u = \frac{1}{2}mv^2$ (4)

$$F(u) = Ap \ln(u/B)/u.$$

The function $F(u)$ is sketched in Fig. 4. We can now find the injection energy, i.e., the minimum value of energy that a fast electron must have to run away from the avalanche and be injected into the decreasing field region ahead of the avalanche. From Eq. (3) the runaway condition is defined as

$$F(u) = eE \qquad (5)$$

and yields the minimum energy u_i for $F(u_i) = eE_m$ (see Fig. 4), where E_m is the maximum field at the front of the avalanche (Fig. 2). Electrons with energy $u \geq u_i$ can run away from the avalanche. Gurevich[20] found that the flux of runaways falls off rapidly with increasing ratio F_{max}/eE, where F_{max} is the maximum value of the retarding force, so that the greatest number of runaway electrons will be found near u_i.

In a reference frame moving with the main avalanche, the energy change of one of these injected electrons per unit distance away from the avalanche front is given by

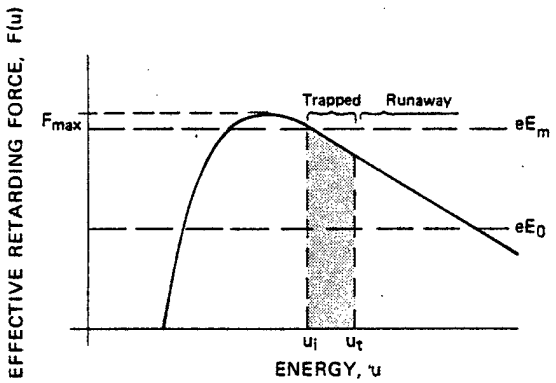

FIG. 4. Effective retarding force as a function of electron energy.

$$du/dx = eE(x) - F(u), \tag{6}$$

where u is the fast electron energy in eV. At $x = 0$, u = injection energy of a given fast electron.

From Eq. (6) and from Fig. 5, we note that an injected particle with energy $u_0 > u_i$ will start to gain energy because $du/dx|_{x=0} > 0$. However, if the rate of energy gained from the field is less than the rate of energy loss due to collisions, the particle will slow down and be trapped. This is due to the fact that the particle is moving in a region of decreasing field with a larger gradient than that of the loss function F.

In (u, x) space, the equation

$$eE(x) = F(u) \tag{7}$$

defines the locus of points for which $du/dx = 0$. A particle, starting with energy u_0, whose trajectory crosses this line will become trapped. Thus there is a range of injected particle energies $u_i < u < u_t$ which will slow down and become trapped. u_t is the injection energy of a particle whose trajectory is tangent to the locus curve [Eq. (7)] for $x \to \infty$. The electrons in this range of energy become trapped at various distances from the avalanche. Thus a narrow channel, as described in Sec. II, evolves from the main avalanche. To show this effect, it is necessary to solve Eq. (6) with $F(u)$ given by Eq. (4). To do so, we must know the dependence of the electric field with x.

It is common practice to assume that the avalanche may be replaced by either a spherical cloud of electrons[2] or by a conducting sphere.[16] We, however, will assume that just prior to stage IV, the avalanche may be represented by a conductor with an excess of electrons. The reasoning is as follows: n_1 electrons after traveling a certain distance produce n_2 ions and n_2 electrons. The $n_1 + n_2$ electrons and n_2 ions act collectively to establish a minimum field configuration inside the avalanche. This configuration can be thought of as being formed by the superposition of a dipole charge distribution (i.e., similar to the uncharged conducting sphere approach) and an electron layer (similar to the electron-cloud approach). The axial field at a distance x from the boundary of the avalanche may then be written as[23]

$$E(x) = E_0 + \tfrac{3}{8}\pi E_0 \left(\frac{r_e}{r_e + x}\right)^2 + 2E_0 \left(\frac{r_e}{r_e + x}\right)^3, \tag{8}$$

where r_e is the radius of the avalanche just prior to the transition into stage IV and E_0 is the applied electric field. As the applied field increases (e.g. 50% overvoltages), the transition to stage IV occurs closer to the cathode. As this happens, the contribution to Eq. (8), due to the $(n_1 - 1)$ ions left behind by the avalanche, must be taken into consideration. Their effect is to reduce the value of the second term in the right-hand side of Eq. (8). At higher fields ($\gtrsim$80% overvoltages), the transition occurs very close to the cathode. For these cases, the whole space charge has a dipole structure so that the second term in Eq. (8) disappears.

Numerical solutions of Eqs. (4), (6), and (8) are shown in Fig. 5 for the case of breakdown in a 1-cm gap in nitrogen at atmospheric pressure. The dotted curve is the locus curve, i.e., Eq. (7). The differences between Figs. 5(a), 5(b), 5(c), and 5(d) are in the values of r_e and E_0 used. In Fig. 6, we show the minimum injection energy u_i as a function of the maximum electric field E_m for this example. The values for the parameters A and B in Eq. (4) were found from the data in.[22]

The results are qualitatively similar: Injected fast electrons with energies in the range $u_i < u < u_t$ become trapped at various distances ahead of the avalanche. Electrons with $u > u_t$ will actually run away. Their number increases as the applied field increases. When $E_m > F_{max}/e$, the runaway flux is substantial. Under these conditions, the fast electron distribution is no longer given by Eq. (3). A solution to the Boltzmann equation when strong electric fields are present must be obtained.

The minimum injection energy and the trapping distance are a function of r_e and E_0. The consequence of this dependence is discussed in the next section.

IV. DISCUSSION

It is impossible to apply a fundamental model alone, as presented in Sec. III, to a specific experiment. In general, each experiment involves the fundamental physical processes and processes related to idiosyncrasies of a particular experiment. It is sometimes difficult to isolate the contribution from each process thus leading to misinterpretation. In the early days of the streamer

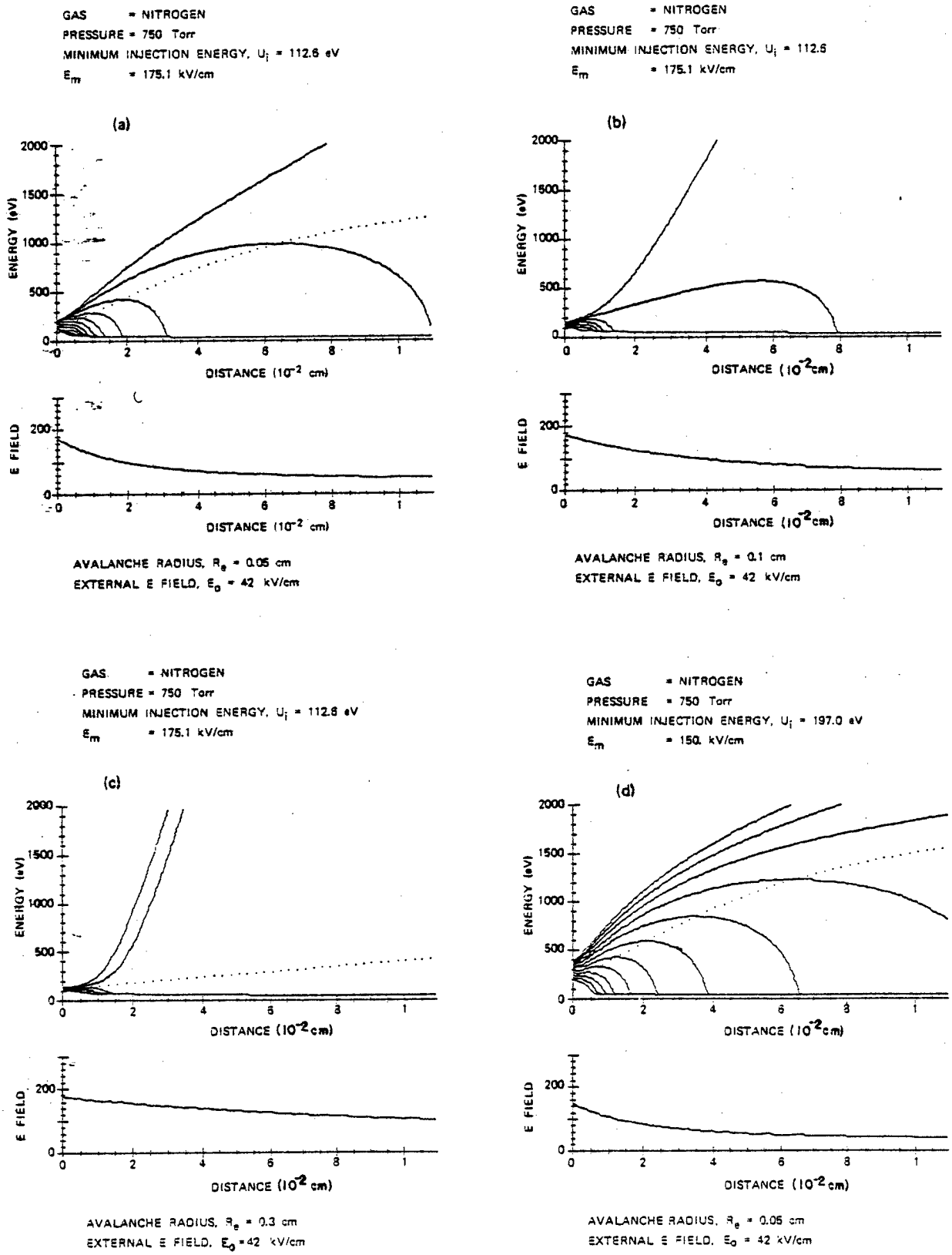

FIG. 5. Evolution of injected electron energy as a function of distance away from the avalanche head.

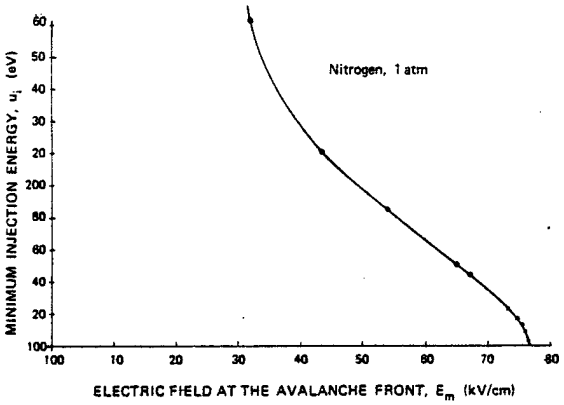

FIG. 6. Minimum injection energy as a function of maximum electric field.

model, Dickey[14] questioned the necessity for introducing a "new" model, besides the Townsend model, to explain the short time lag experimentally observed by Rogowski[10] and later by Fletcher.[11] He argued that these time lags were due to the particular experimental arrangement and not due to any new physics in the breakdown process.

In the discussion of our model, we will concentrate on the general structure of the observed breakdowns. We will also examine the transitions that may occur in any specific experimental arrangement due to the fundamental processes in the gas alone.

In the regime of interest to our model (i.e., $V > 20\%$ self-breakdown), two kinds of breakdown development have been observed: (1) filamentary breakdown and (2) broad breakdown. Broad breakdown has been observed either at very large voltages[17] ($V > 2$ times self-breakdown) or at lower voltages when the initiating electrons are generated over a large surface of the cathode.[24] In all other cases, filamentary breakdown occurs.

The principal parameters that we need to describe the structure of the breakdown are (1) the applied electric field E_0, (2) the spatial dependence of the electric field just ahead of the avalanche, and (3) the frictional force, $F(u)$, on an electron as a function of its energy for a given gas. Note that $F(u)$ also depends on the pressure. From Fig. 5 we note that if the avalanche is initially small in cross section (this occurs when the electrons initiating the avalanche are generated in a small area of the cathode), the inhomogeneity in the electric field is large. This implies that the energy spectrum of the trapped electrons is broad, i.e., many electrons will be trapped. Moreover, these electrons will be injected along the axis due to the "escape cone" phenomenon. This behavior corresponds to the range of parameters where filamentary breakdown has been observed.

As the field is increased, we reach the regime described by Mesyats' avalanche chain model.[18] He proposed that the main avalanche slows down and that a new avalanche develops from the previous one. This process is repeated a number of times until an avalanche chain is formed.

In our model, the process is continuous. At the higher field values, the width of the energy spectrum of the trapped electrons decreases due to the fact that the decrease in the injection energy u_i will be smaller than the decrease on the lower energy limit for runaway, i.e., u_t. Accordingly, the range of the trapped electrons decreases. The avalanche is extended via these short-range electrons [see Fig. 5(a)]. The number of runaway electrons and their effect in this regime is still small. However, as the field increases further (i.e. $\gtrsim 2$ times self-breakdown), the injected electrons are no longer trapped. In this regime $eE(x) > F(u(x))$ and electrons continuously gain energy; they all run away [compare Figs. 5(a) and 5(d)]. This is the regime discussed by Babic *et al.*[16] Our model is, in this regime, similar to theirs; however, we do not assume that the injected electrons have zero initial velocity and we are consistent in our definition of runaway electrons. This discharge in this regime has a diffuse or multichannel character.

A situation similar to the above, i.e., no trapped electrons, exists when the breakdown is initiated by a large number of electrons distributed over a large area.[24] In this case, the inhomogeneity ahead of the avalanche is small so that once again injected electrons actually runaway [see Fig. 5(c)]. The result, as in the very high field conditions, is a broad breakdown due to ionization and radiation generated by these runaways.

A subject of interest has been whether or not an abrupt decrease in the formative time would be observed as the percent overvoltage above self-breakdown is increased. In this respect the results have been mixed.[25] In some cases, in oxygen, and nitrogen, for example, a decrease was observed for large gap spacing. In hydrogen, however, it was not. This behavior can be explained by considering the magnitude of the maximum of the retarding force for each gas and the percent overvoltage used. The number of injected electrons is a function of E_{cr}, where $E_{cr} = F_{max}/e$ (see Fig. 4).[20] If $E_m \ll E_{cr}$ (see Sec. III) the number of injected electrons is practically zero so that no transition will be observed. As E_m increases, the number of injected electrons increases. Accordingly a continuous change in the slope of the time lag versus percent overvoltage curve may be observed. This was observed experimentally by Phillip and Allen.[25] We were not able to check our

model for all the gases they used due to lack of data on the frictional force. For the cases of hydrogen, oxygen, and nitrogen, for which data is available, the observed time lag versus overvoltage curve may be explained by our model.

In the case of hydrogen, the applied overvoltages used were too low, so that no change in the slope was observed. The maximum of the retarding force for hydrogen is relatively high, while the breakdown voltage for a 1-cm gap is small (i.e., ~15 kV). Therefore, large percentage overvoltages (~3 times self-breakdown) will be required before injection can begin.

For the cases of oxygen and nitrogen, changes were observed for a 3-cm gap at atmospheric pressure. The changes were more pronounced in oxygen than in nitrogen. The maximum retarding force for oxygen is less than for nitrogen; moreover, the breakdown voltage for oxygen is higher. This combination may account for the observed differences.

As the gap width decreased for the same range of overvoltages, the change in the slope decreased. For a gap width of 1 cm, no change was observed in nitrogen for up to 25% overvoltages. As for hydrogen, these values are again too low for injection to occur. No experiments were performed for oxygen in 1-cm gaps although the trend seems to indicate that a similar behavior would be obtained. The changes observed for 3-cm gaps in these two gases at these lower overvoltages may be due to large space-charge distortion which lowers the injection energy. This may occur if the magnitude of the "free charge" just prior to stage IV is large (see Sec. III), in which case the second term in Eq. (8) will be larger.

The next step in the development of the model is to do a numerical analysis of a fluid model for various particle species. The important point is that the electron fluid must be divided into two groups: the fast and slow electrons. A number of experiments should be carried out to test the validity of the theory and its basic assumptions. In particular, since the retarding force in Eq. (6) is a function of the properties of the gas,[21] the appearance of the runaway electrons will depend strongly on the gas used. A series of experiments should be carried out to test this dependence. Moreover, experimental verification of the time of appearance of the runaway electrons as a function of percent overvoltage should be provided.

ACKNOWLEDGMENTS

We wish to express appreciation to Professor G. A. Mesyats and Professor M. O. Hagler for stimulating discussions, and to Dr. B. D. Blackwell for his assistance with the computer graphics. We also want to thank the reviewer for suggesting, among other things, changes in the title of the paper to its present form. This work was supported by the Naval Surface Weapon Center under Contract No. N60921-79C-A187 and in part by the Air Force Office Scientific Research under Contract No. AFOSR 76-3124A. The findings in this paper are not to be construed as an official Department of Navy position unless so designated by other authorized documents.

[1] F. Llewellyn-Jones, *Ionization and Breakdown in Gases* (Methuen, London, 1966), p. 50.
[2] H. Raether, *Electron Avalanches and Breakdown in Gases* (Butterworths, London, 1964).
[3] J. Dutton and W. T. Morris, Br. J. Appl. Phys. 18, 1115 (1967).
[4] L. H. Fisher and B. Bederson, Phys. Rev. 81, 109 (1951).
[5] A. J. Davies, C. J. Evans, and P. M. Woodison, Comput. Phys. Commun. 14, 287 (1978).
[6] A. J. Davies, C. J. Evans, and F. Llewellyn-Jones, Proc. R. Soc. London A281, 164 (1964).
[7] A. L. Ward, Phys. Rev. 138, 1357 (1965).
[8] G. M. Petropoulos, Phys. Rev. 78, 250 (1950).
[9] E. D. Lozanskii, Zh. Tekh. Fiz. 38, 1563 (1968) [Sov. Phys.—Tech. Phys. 13, 1269 (1969)].
[10] W. Rogowski, Archiv Electrotech. (Berlin) 20, 235 (1928).
[11] R. C. Fletcher, Phys. Rev. 76, 1501 (1949).
[12] F. Llewellyn-Jones, *Ionization and Breakdown in Gases* (Methuen, London, 1966), p. 149.
[13] G. A. Mesyats, Y. I. Bychkov, and A. I. Iskol'dskii, Zh. Tekh. Fiz. 38, 1281 (1968) [Sov. Phys.—Tech. Phys. 13, 1051 (1969)].
[14] F. R. Dickey, Jr., J. Appl. Phys. 23, 1336 (1952).
[15] Y. L. Stankevich and V. G. Kalinin, Dokl. Akad. Nauk SSSR 177, 72 (1967) [Sov. Phys.—Dokl. 12, 1042 (1968)].
[16] L. P. Babich and Y. L. Stankevich, Zh. Tek. Fiz. 42, 1669 (1972) [Sov. Phys.—Tech. Phys. 17, 1333 (1973)].
[17] L. V. Tarasova, L. N. Khudyakova, T. V. Loiko, and V. A. Tsukerman, Zh. Tekh. Fiz. 44, 564 (1974) [Sov. Phys.—Tech. Phys. 19, 351 (1974)].
[18] V. V. Kremnev and G. A. Mesyats, Zh. Prikl. Mekh. Tekh. Fiz. 1 [J. Appl. Mech. Tech. Phys. (USSR) 40 (1971)].
[19] E. D. Lozanskii, Usp. Fiz. Nauk. 117, 493 (1975) [Sov. Phys.—Usp. 18, 893 (1976)].
[20] A. V. Gurevich, Zh. Eksp. Teor. Fiz. 39, 1296 (1960) [Sov. Phys.—JETP 12, 904 (1961)].
[21] L. D. Landau and E. M. Lifshitz, *Electrodynamics of Continuous Media* (Pergamon, London, 1966), p. 344.

[22]L. R. Peterson and A. E. S. Green, J. Phys. B 1, 1131 (1968).
[23]J. A. Stratton, *Electromagnetic Theory* (McGraw-Hill, New York, 1941), p. 205.
[24]J. Koppitz, J. Phys. D 6, 1494 (1973).
[25]K. R. Allen and K. Phillips, Proc. Roy. Soc. London A278, 188 (1963).

THIRTY-THIRD GASEOUS ELECTRONICS CONFERENCE

7-10 October 1980

Norman, Oklahoma

PLEASE TYPE NAME & ADDRESS

E.E. Kunhardt
Ionized Gas Laboratory
Texas Tech University
P.O. Box 4439
Lubbock, Texas 79409

DO NOT WRITE IN THIS SPACE

Serial No. _____

Accepted: Yes ____ No ____

Session _____

Number _____

Date Conf. _____

AUTHORS PLEASE NOTE

Indicate in what subject category your paper best belongs (see preliminary announcement for category)

1 2 3 4 5 6
(7) 8 9 10 11 12
13 14 15

Development of Overvoltage Breakdown at High Gas Pressure - E.E. KUNHARDT and W.W. BYSZEWSKI, Texas Tech University* -- A model for the development of electrical breakdown in high pressure gases is presented. It describes the initial phases of breakdown in the regime where the Townsend avalanche mechanism does not apply. In the model, the energy distribution function for electrons in the advancing avalanche is assumed to have two components: The fast and the slow electrons. The fast electrons "runaway" from the avalanche, but are "trapped" at various distances ahead of the avalanche, depending on the energy of the electrons and the properties of the avalanche and the background gas. This mechanism plays the fundamental role in increasing the speed of propagation of the avalanche when the applied voltage is $\geq$ 20 percent of the self breakdown voltage. In light of this model a brief discussion of experimental results if given.

* This work was supported by the Naval Surface Weapons Center, Dahlgren, Va, under contract No. N60921-79-C-A187 and in part by the Air Force Office of Scientific Research under Contract No. AFOSR 76-3124A.

Appendix III

Numerical Solution of Poisson's Equation

Numerical Solution of Poisson's Equation in Cylindrical Coordinates Using FFT and Cubic Splines

E. E. Kunhardt

Ionized Gas Laboratory

Texas Tech University

Objective: to solve $\frac{1}{r}\partial_r (r\,\partial_r \phi) + \partial_z^2 \phi = -4\pi\rho$ (1)

with boundary conditions:

$\phi = 0$ @ $z = 0$ (cathode)

$\phi = 0$ @ $z = d$ (anode)

$\partial_r \phi = 0$ @ $r = 0$

and $\phi = 0$ @ $r = r_b$

Where r_b is the "furthest radius" of interest. (2)

Motivation: The above "mathematical" problem is applicable to the "physical" problem of finding the values of electric field in a gap due to the space charge in the gap. Cylindrical symmetry (which is not a major restriction) is assumed.

Importance: A major obstacle in tracking the space-time development of the breakdown of an overvolted gap is the time (computational) required to solve the Poisson equation. A fast alogarithm will result in large savings of time, which in turn implies that we will be able to track the development of the breakdown for a longer period of time.

Results: We have developed a direct alogarithm for solving Poisson's Equation in Cylindrical coordinates.

Technique:

1. Apply Fourier transform in z, making use of the FFT alogarithm.[1]
2. Use Cubic Splines to solve for the fourier coefficients as a function of r.
3. Directly obtain the electric field by inversion of appropriate spline coefficient.

Description of Technique:

Let

$$\phi(r,z) = \sum_k \phi_k(r) \sin \frac{k\pi}{d} z$$

and

$$\rho(r,z) = \sum_k \rho_k(r) \sin \frac{k\pi}{d} z$$

Substituting into Equation (1) and using the orthogonality properties of the sine functions in the interval $0 \leq z \leq d$, we get:

$$\frac{d^2}{dr^2} \phi_k(r) + \frac{1}{r} \frac{d}{dr} \phi_k(r) - \left(\frac{\pi k}{d} \right)^2 \phi_k(r) = -4\pi\rho_k(r) \qquad (3)$$

Equation (3) is a set of k equations since we only need k harmonics i.e. equal to the number of grid points in z.

The boundary conditions that go with Equation (3) are:

$$\partial_r \phi_k = 0 \qquad @ \qquad r = 0$$

$$\phi_k(r_b) = 0$$

Since the developing avalanche has a very small radius ($\sim$ .1 cm), it is desirable to expand the region around the origin (r = 0) by using a trans-

formation of coordinates in the r direction. A transformation which will suit our purpose is:

$$\zeta = a(1 - e^{-br}) \tag{4}$$

Where a and b are parameters chosen so as to provide the desirable expansion around the axis. Note that for $o \leq r \leq \infty$; the ζ range is $0 \leq \zeta \leq a$. Using the transformation in (4), Equation (3) becomes:

$$\frac{d^2}{d\zeta^2} \phi_k(\zeta) + p(\zeta) \frac{d}{d\zeta} \phi_k(\zeta) - q(\zeta) \phi_k(\zeta) = -S(\zeta) \tag{5}$$

Where

$$p(\zeta) = - \frac{\ln \left(\frac{a-\zeta}{a} \right) + 1}{\ln \left(\frac{a-\zeta}{a} \right)} \frac{1}{a-\zeta}$$

$$q(\zeta) = + \left(\frac{\pi k}{d}\right)^2 \frac{1}{b^2(a-\zeta)^2} \quad \text{and} \quad S(\zeta) = \frac{4\pi\rho k}{b^2 (a-\zeta)^2}$$

Equation (5) is valid everywhere except for $\zeta = 0$. Taking the limit as $\zeta \to 0$, we obtain:

$$\frac{d^2}{d\zeta^2} \phi_k(0) - \left(\frac{\pi k}{d}\right)^2 \frac{1}{2b^2a^2} \phi_k(0) = \frac{-2\pi\rho k(0)}{b^2a^2} \tag{6}$$

To solve Eqs. (5) and (6), define the cubic spline as a function $G(\zeta) \in C_2$ $[0,\zeta_b]$, of the form, in each of the subintervals $[\zeta_i, \zeta_{i+1}]$:[2]

$$G_i(\zeta) = G_{o,i} + G_{1,i} (\zeta-\zeta_i) + \frac{1}{2} G_{2,k}(\zeta-\zeta_i)^2 + \frac{1}{6} G_{3,i} (\zeta-\zeta_i)^3 \tag{7}$$

where $G_{n,i}$ are constants.

Now we define the system of Eqs. for $G_{n,i}$, $n = 0, 1,2,3$; $i = 0,1,....N$; such that Eq. (7) satisfies Eq. (5) and (6) at the points $\zeta_o,....., \zeta_{n+1}$ and $G(\zeta)$, $\underline{G}'(\zeta)$, $G''(\zeta)$ are continuous at the points $\zeta_k,....., \zeta_n$[2].

From Eq. (7), we get:

$$G_i(\zeta_i) = G_{o,i} \tag{8}$$

$$\partial_\zeta G_i(\zeta_i) = G_{1,i} \tag{8b}$$

$$\partial^2_\zeta G_i(\zeta_i) = G_{2,i} \tag{8c}$$

The grid structure in ζ is shown below.

$$\underset{\zeta_o = 0}{G_o} \quad \underset{\zeta_1}{G_1} \quad \cdots\cdots \quad \underset{\zeta_{i-1}}{G_{i-1}} \quad \underset{\zeta_i}{G_i} \quad \cdots\cdots \quad \underset{\zeta_{n-1}}{G_{n-1}} \quad \underset{\zeta_n}{G_n} \quad \underset{\zeta_b}{}$$

Applying continuity requirements at ith point:

a) $G_i(\zeta_i) = G_{i-1}(\zeta_i)$ (9)

Noting that:

$$G_{i-1}(\zeta_i) = G_{o,i-1} + G_{1,i-1} + \Delta\zeta_{i-1} + G_{2,i-1} \frac{\Delta\zeta^2_{i-1}}{2} + G_{3,i-1} \frac{\Delta\zeta^3_{i-1}}{6} \quad (10a)$$

$$\partial_\zeta G_{i-1}(\zeta_i) = G_{1,i-1} + G_{2,i-1} + G_{2,i-1}\,\Delta\zeta_{i-1} + G_{3,i-1}\,\frac{\Delta\zeta^2_{i-1}}{2} \quad (10b)$$

where $\Delta\zeta_{i-1} = \zeta_i - \zeta_{i-1}$

Using (8a), (9), and (10a),

$$G_{o,i} = G_{o,i-1} + G_{1,i-1}\Delta\zeta_{i-1} + G_{2,i-1}\,\frac{\Delta\zeta^2_{i-1}}{2} + G_{3,i-1}\,\frac{\Delta\zeta^3_{i-1}}{6} \quad (11)$$

b) $\partial_\zeta G_i(\zeta_i) = \partial_\zeta G_{i-1}(\zeta_i)$ (12)

Using (8b), (10b), and (12):

$$G_{1,i} = G_{1,i-1} + G_{2i-1}\,\Delta\zeta_{i-1} + G_{3,i-1}\,\frac{\Delta\zeta^2_{i-1}}{2} \quad (13)$$

c) $\partial^2_\zeta\, G_i(\zeta_i) = \partial^2_\zeta\, G_{i-1}\,(\zeta_i)$ (14)

Using (8c), (10c), and (14)

$$G_{2,1} = G_{2,i-1} + G_{3,i-1}\,\Delta\zeta_{i-1} \quad (15)$$

Equations (11), (13), and (15) are valid for the points i = 1 ·---N.

Besides these continuity equations, the spline functions must satisfy the differential equation at each point. From equations (5) and (6) and equations (8):

$$G_{2,i} + p(\zeta_i)\, G_{1,i} + q(\zeta_i)\, G_{1,i} = S(\zeta_i) \qquad i \neq 0$$

The above equation is re-written as:

$$G_{2,i} + p_i\, G_{1,i} - q_i\, G_{0,i} = -S_i \tag{16}$$

where $p_i = p(\zeta_i)$ $\quad i \neq 0$

$= 0$ $\quad i = 0$

$q_i = q(\zeta_i)$ $\quad i = 0, \ldots N+1$

$S_i = S(\zeta_i)$ $\quad i = 0, \ldots N+1$

Using Equations (11), (13), (15), and (16), we obtain the following Equation for $G_{1,i}$ (after considerable algebra):

$$[\, A_{i+1}\, D_i A_i \,]\, G_{1,i+1} = [\, B_{i+1}\, C_i A_i + C_{i+1}\, A_i b_i + C_{i+1}\, C_i c_i \,]\, G_{1,i}$$
$$- [\, C_{i+1}\, B_i b_i + C_{i+1}\, C_i d_i \,]\, G_{1,i-1} + [\, D_{i+1}\, C_i A_i \,]\, S_{i+1}$$
$$+ [\, E_{i+1}\, C_i A_i - C_{i+1}\, D_i b_i - C_{i+1}\, C_i e_i \,]\, S_i$$
$$- [\, C_{i+1}\, E_i b_i + C_{i+1}\, C_i f_i \,]\, S_{i-1} \tag{17}$$

for $i = 1, \ldots\ldots, N$

Note that from boundary conditions and equation (8b):

$$G_{1,o} = G_{1,N+1} = 0$$

That is, the radial field is zero on the axis and at ζ_b.

Equation (17) is a tridiagonal system of equations for $G_{1,i}$ which can be inverted using standard computational techniques. The constants A, B, C, D, E, and a , b, c, d, e, f are given by:

$$A_i = 1 + \frac{\Delta\zeta_{i-1}}{2}\, p_i - \frac{\Delta\zeta_{i-1}}{2}\, \frac{q_1 C_i}{a_i} \qquad E_i = \frac{\Delta\zeta_{i-1}}{2} - \frac{\Delta\zeta_{i-1}}{2}\, \frac{q_i f_i}{a_i}$$

$$B_i = 1 - \frac{\Delta\zeta_{i-1}}{2}\, p_{i-1} - \frac{\Delta\zeta_{i-1}}{2}\, \frac{q_i d_i}{a_i} \qquad a_i = 1 + \frac{\Delta\zeta^2_{i-1}}{6}\, q_i$$

$$C_i = \frac{\Delta\zeta_{i-1}}{2}\, q_{i-1} + \frac{\Delta\zeta_{i-1}}{2}\, \frac{q_i b_i}{a_i} \qquad b_i = 1 - \frac{\Delta\zeta^2_{i-1}}{3}\, q_{i-1}$$

$$D_i = \frac{i-1}{2} - \frac{i-1}{2}\, \frac{q_i e_i}{a_i} \qquad c_1 = \frac{2}{i-1}\, p_i$$

$$d_i = \Delta\zeta_{i-1} - \frac{\Delta\zeta^2_{i-1}}{3} \; p_{i-1}$$

$$e_i = \frac{\Delta\zeta^2_{i-1}}{6}$$

$$f_i = \frac{\Delta\zeta^2_{i-1}}{3}$$

Note from equation (8b) that $G_{1,i}(\zeta_i)$ is the fourier transform of the radial Electric field, so we need not find any of the other coefficients. Inverting $G_{1,i}(\zeta_i)$, we obtain the radial field. The inverse cosine transform of $K\, G_{0,i}$ gives us the axial field.

References:

1. R. W. Hockney, J. of the Assc. for Comp. Mach. 12, 95 (1965).

2. V. P. Il'in, U.S.S.R. Comp. Meth. Math. Phys. 18, 92 (1978).

Sine and Cosine transform subroutines

and Spline subroutines.

The subroutines FFT(N, X, Itype1, Itype2) and spline are used to solve the Poisson equation in cylindrical cooordinates with axial symmetry. The procedure is as follows:

Given a space charge p(r); the forward sine transform is taken (i.e. Itype1 = 1, Itype2 = -1). Then the radial equation (Eq. 3 of outline) is solved for each fourier component using subroutine spline. The space charge is brought into the subroutine as ER(I, K). Use is made again of the FFT to obtain the radial field and the longitudinal field at each radial point, as a function of z (axial coordinates), via inverse transformation (Itype2 = 1). Note: The Spline subroutine shown does not use coordinate transformation. For this case $p_i(\zeta)$ in Eq. 5 is given by $1/r_i$ and $q_i(\zeta)$ is given by $(\frac{\pi k}{d})^2$.

```
      SUBROUTINE FFT(N,X,ITYPE1,ITYPE2)
C
C
C     SUBROUTINE FOR FFT USED IN COMPUTING SINE OR COSINE TRANSFORMS
C
C     NOTE : 2**N=2*(NZ-1), IE. SIGNAL HAS (2**(N-1)+1 POINTS
C
C     ITYPE1: -1 FOR COS TRANSFORM, 1 FOR SIN TRANSFORM
C
C     ITYPE2: 1 FOR INVERSE TRANSFORM, -1 FOR FORWARD TRANSFORM
C
C
      TYPE COMPLEX W,FBUF,Z,CMPLX,W1
      COMMON/FT/W(256),W1(256)
      DIMENSION FBUF(512),Z(512),X(128)
      NT=2**N
      AN=NT
      NH=NT/2
      NH1=NH+1
C
C     CHECK IF FORWARD OR INVERSE
C
      IF(ITYPE2.GE.0) 10,40
   10 CONTINUE
      IF(ITYPE1 .GE.0) 20,40
   20 CONTINUE
C
C     TRANSFER DATA TO FBUF COMPLEX ARRAY
C
      FBUF(1)=CMPLX(0.,X(1))
      DO 30 I=2,NH1
      FBUF(I)=CMPLX(0.,X(I))
      FBUF(NT+2-I)=-FBUF(I)
   30 CONTINUE
      GO TO 80
   40 CONTINUE
      FBUF(1)=CMPLX(X(I),0.)
      DO 110 I=2,NH1
      FBUF(I)=CMPLX(X(I),0.)
C
C     CHECK IF SINE OR COSINE
C
      IF(ITYPE1.GE.0) 390,400
  390 CONTINUE
      FBUF(NT+2-I)=-FBUF(I)
C
C      NOTE THAT FBUF(NT/I+1)=0.
C
      GO TO 110
  400 FBUF(NT+2-I)=FBUF(I)
  110 CONTINUE
   80 CONTINUE
C
C    DO STUFF
C
      DO 250 K=1,N
```

```
      M=2**(K-1)
      L=2*M
C
      DO 215 I=1,NT,L
      ILM=I/L*M
C
      DO 200 J=1,M
  200 Z(I+J-1)=FBUF(ILM+J)+FBUF(ILM+J+NH)
C
C
      DO  210 J=1,M
C
C     CHECK IF FORWARD OR INVERSE
C
      IF(ITYPE2 .GE. 0) 410,420
  420 Z(I+J+M-1)=(FBUF(ILM+J)-FBUF(ILM+J+NH))*W(ILM+1)
      GO TO 210
  410 Z(I+J+M-1)=(FBUF(ILM+J)-FBUF(ILM+J+NH))*W1(ILM+1)
  210 CONTINUE
  215 CONTINUE
      DO 220 I=1,NT
  220 FBUF(I)=Z(I)
  250 CONTINUE
C
C     CHECK IF FORWARD OR INVERSE
C
      DO 600 I=1,NH1
      IF(ITYPE2.GE.0)270,280
  270 CONTINUE
      FBUF(I)=FBUF(I)/AN
      GO TO 540
  280 CONTINUE
C
C     CHECK IF SINE OR COSINE
C
      IF(ITYPE1.GE.0)530,540
  530 X(I)=AIMAG(FBUF(I))
      GO TO 600
  540 X(I)=REAL(FBUF(I))
  600 CONTINUE
      RETURN
      END
```

```
      SUBROUTINE SPLINE
C
C       THIS SUBROUTINE EVALUATES THE RADIAL EQUATION USING  SPLINES
C
C
C     ALL CONSTANTS NEEDED IN THIS SUBROUTINE ARE CALCULATED
C     IN THE MAIN PROGRAM AND ARE COMMON WITH THIS SUBROUTINE
C
      DIMENSION PHI(64,64),ER(64,64),EZ(64,64)
      DIMENSION ORG1(128),ORG2(128),ORG3(128)
      DIMENSION ALPHA(128),SI(128),B(128)
      EQUIVALENCE(PHI,EZ)
      COMMON ER,EZ
      COMMON/A/R0,Z0,NR,NZ/B/DR,DRZ,DRS,DRS6
      COMMON/C/NR1,NRM1,NRM2
      COMMON/D/ITV,PI
C
C       R0 IS THE LENGTH IN THE R DIRECTION, Z0 IS THE LENGTH INTHE
C     Z DIRECTION.
C     DR IS THE STEP SIZE IN R
C       DR2=DR/2.
C     DRS=DR*DR
C     DRS6=DRS/6.
C     NR+1 IS THE TOTAL NUMBER OF POINTS IN R.
C     NR1=NR+1
C       NRM1=NR-1
C     NRM2=NR-2
CC    ITV IS THE EIGEN VALUE IN THE Z DIRECTION (I.E. K IN SINE EXPANSI
C
C
      EV=ITV*PI/Z0
C
C     DO LAST POINT IN TRIDIAGONAL FACTORIZATION
C
      I=NRM1
      DRST0=(I-1)*DR
      DRST1=I*DR
      DRST=(I+1)*DR
      P2=1./DRST
      P1=1./DRST1
      P0=1./DRST0
      Q1=EV*EV
      Q0=Q1
      Q2=Q1
C
      AS1=1.-Q1*DRS6
      BS1=1.+Q0*2.*DRS6
      CS1=DRS6*P1
      DS1=DR-2.*DRS6*P0
      ES1=DRS6
      FS1=2.*DRS6
C
      AL1=1.+DR2*P1+CS1*Q1*DR2/AS1
      BL1=1.-DR2*P0+DS1*DR2*Q1/AS1
      CL1=DR2*Q0+BS1*DR2*Q1/AS1
      DL1=DR2+ES1*DR2*Q1/AS1
```

```
      EL1=DR2+FS1*DR2*Q1/AS1
C
      AS2=1.-Q2*DRS6
      BS2=1.+2.*DRS6*Q1
      CS2=DRS6*P2
      DS2=DR-2.*DRS6*P1
      ES2=ES1
      FS2=FS1
C
      AL2=1.+DR2*P2+CS2*DR2*Q2/AS2
      BL2=1.-DR2*P1+DS2*DR2*Q2/AS2
      CL2=DR2*Q1+BS2*DR2*Q2/AS2
      DL2=DR2+ES2*DR2*Q2/AS2
      EL2=DR2+FS2*DR2*Q2/AS2
C
      A=AS1*BL2/CL2+BS1*AL1/CL1-CS1
      N=I+1
      B(N)=DS1-BS1*BL1/CL1
      S0=FS1-BS1*EL1/CL1
      S1=AS1*EL2/CL2+ES1-BS1*DL1/CL1
      F2=S1*ER(NR,ITV)+S0*ER(NRM1,ITV)
      ALPHA(N)=A
      SI(N)=F2
      GAMMA=0.
      ORG1(N+1)=AL2/CL2
      ORG2(N+1)=-BL2/CL2
      ORG3(N+1)=EL2*ER(NRM1,ITV)/CL2
C
C     EVALUATE INTERMIDIATE POINTS IN THE TRIDIAGONAL EQUATION
C
      DO 2010 I=2,NRM2
      NF=NR-I
      P1=P0
      Q1=Q0
      AS2=AS1
      BS2=BS1
      CS2=CS1
      DS2=DS1
      ES2=ES1
      FS2=FS1
C
      AL2=AL1
      BL2=BL1
      CL2=CL1
      DL2=DL1
      EL2=EL1
C
      DRST0=(NF-1)*DR
      P0=1./DRST0
      Q0=Q1
C
      AS1=1.-Q1*DRS6
      BS1=1.+Q0*2.*DRS6
      CS1=DRS6*P1
      DS1=DR-2.*DRS6*P0
      ES1=DRS6
```

```
      FS1=2.*DRS6
C
      AL1=1.+DR2*P1+CS1*Q1*DR2/AS1
      BL1=1.-DR2*P0+DS1*DR2*Q1/AS1
      CL1=DR2*Q0+BS1*DR2*Q1/AS1
      DL1=DR2+ES1*DR2*Q1/AS1
      EL1=DR2+FS1*DR2*Q1/AS1
C
      GAMMA=-AS1*AL2/CL2/ALPHA(NF+2)
      C=-AS1*AL2/CL2
      A=AS1*BL2/CL2+BS1*AL1/CL1-CS1
      N1=NF+1
      ALPHA(N1)=A-GAMMA*B(N1+1)
      B(N1)=DS1-BS1*BL1/CL1
      S0=FS1-BS1*EL1/CL1
      S1=AS1*EL2/CL2+ES1-BS1*DL1/CL1
      S2=AS1*DL2/CL2
      F2=S2*ER(NF+2,ITV)+S1*ER(NF+1,ITV)+S0*ER(NF,ITV)
      SI(N1)=F2-GAMMA*SI(N1+1)
      ORG1(N1+1)=AL2/CL2
      ORG2(N1+1)=-BL2/CL2
      ORG3=DL2*ER(N1+1,ITV)/CL2+EL2*ER(N1,ITV)/CL2
C
 2010 CONTINUE
C
C
C     DO FIRST POINT
C
      I=1
      P1=P0
      Q1=Q0
      AS2=AS1
      BS2=BS1
      CS2=CS1
      ES2=ES1
      FS2=FS1
      AL2=AL1
      BL2=BL1
      CL2=CL1
      DL2=DL1
      EL2=EL1
      P0=0.
      Q0=Q1/2.
C
      AS1=1.-Q1*DRS6
      BS1=1.+Q0*2.*DRS6
      CS1=DRS6*P1
      DS1=DR-2.*DRS6*P0
      ES1=DRS6
      FS1=2.*DRS6
      AL1=1.+DR2*P1+CS1*Q1*DR2/AS1
      BL1=1.-DR2*P0+DS1*DR2*Q1/AS1
      CL1=DR2*Q0+BS1*DR2*Q1/AS1
      DL1=DR2+ES1*DR2*Q1/AS1
      EL1=DR2+FS1*DR2*Q1/AS1
C
```

```
      C=-AS1*AL2/CL2
      GAMMA=-AS1*AL2/CL2/ALPHA(3)
      A=AS1*BL2/CL2+BS1*AL1/CL1-CS1
      ALPHA(2)=A-GAMMA*B(3)
      B(2)=0.
      S0=FS1-BS1*EL1/CL1
      S1=AS1*EL2/CL2+ES1-BS1*DL1/CL1
      S2=AS1*DL2/CL2
      F2=S2*ER(3,ITV)+S1*ER(2,ITV)+S0*ER(1,ITV)
      ORG1(3)=AL2/CL2
      ORG2(3)=-BL2/CL2
      ORG3(3)=DL2*ER(3,ITV)/CL2+EL2*ER(2,ITV)/CL2
      ORG1(2)=AL1/CL1
      ORG2(2)=-BL1/CL1
      ORG3(2)=DL1*ER(2,ITV)/CL1+EL1*ER(2,ITV)/CL1
      SI(2)=F2-GAMMA*SI(3)
      ER(2,ITV)=SI(2)/ALPHA(2)
C
C
C
C
C     EVALUATE THE TRANSFORMED RADIAL FIELD
C
      DO 2020 I=3,NR
      ER(I,ITV)=(SI(I)-B(I)*ER(I-1,ITV))/ALPHA(I)
 2020 CONTINUE
      ER(1,ITV)=0.
      ER(NR1,ITV)=0.
      PHI(NR1,ITV)=0.
C
C     EVALUATE THE POTENTIAL THEN THE TRANSFORM OF THE LONGITUDINAL FIEL
C
      DO 2022 I=1,NR
      NF=NR1-I
      PHI(NF,ITV)=ORG1(NF+1)*ER(NF+1,ITV)+ORG2(NF+1)*ER(NF,ITV)+ORG3(
     2NF+1)
      EZ(NF,ITV)=EV*PHI(NF,ITV)
 2022 CONTINUE
      RETURN
      END
```

Appendix IV

Abstract of paper on experimental results given at the 33rd Gaseous Electronics Conference.

THIRTY-THIRD GASEOUS ELECTRONICS CONFERENCE

7-10 October 1980

Norman, Oklahoma

PLEASE TYPE NAME & ADDRESS

E.E. Kunhardt
Ionized Gas Laboratory
Texas Tech University
P.O. Box 4439
Lubbock, Texas 79409

DO NOT WRITE IN THIS SPACE

Serial No. _____

Accepted: Yes ____ No ____

Session _____

Number _____

Date Conf. _____

AUTHORS PLEASE NOTE

Indicate in what subject category your paper best belongs (see preliminary announcement for category)

1 2 3 4 5 6
(7) 8 9 10 11 12
13 14 15

Nanosecond-Pulse Breakdown in Gases at High Overvoltages - E.E. KUNHARDT, S. LEVINSON, and M. ALLEY, Texas Tech University* -- Physical insight into the breakdown initiation processes and the formation time of nanosecond-pulse discharges in a homogeneous-field gap may be inferred from the study of the observational delay time. In this paper, we report the results of experiments carried out to measure the observational delay time as a function of gas pressure (up to 1600 Torr) and percent overvoltage (up to 1200%). The experiments were carried out in an evacuable spark gap chamber that forms part of a coaxial line system. Trapezoiday voltage pulses in the range of 50 to 160 kV and 50 ns duration, with 4 ns risetime were applied to the gap. The electrode separation can be varied up to 3 cm. Briefly, the results indicate that there is a minimum in the mean delay time as a function of percent overvoltage. This implies that there are conditions of overvoltage for which avalanche development is optimum. The implication of these results as to the nature of the pre-breakdown processes will be discussed.

* This work was supported by the Naval Surface Weapons Center, Dahlgren, Va. under Contract No. N60921-79-C-A187.

References

1. Trolan, J. K., Charbonnier, F. M., Collins, F. M., and Guenther, A. H., Exploding Wires III, pp. 361-389 (1964).

2. Dakin, T. W., Luxa, G., Opperman, G., Vigreux, J., Wind, G., and Winkelnkemper, H., Electra 32, 61 (1974).